Spring 1981

Structure and properties of neodymium chromite

David Charles Hitchcock

Department:

STRUCTURE AND PROPERTIES OF NEODYMIUM CHROMITE

BY

DAVID CHARLES HITCHCOCK, 1956-

A THESIS

Presented to the Faculty of the Graduate School of the

UNIVERSITY OF MISSOURI-ROLLA

In Partial Fulfillment of the Requirements for the Degree

MASTER OF SCIENCE IN CERAMIC ENGINEERING

1981

Approved by:

Harlan K Anderson (Advisor

L E Moore

Edward B. Hale

ABSTRACT

Pure, accepton and Al doped $NdCrO_3$ were prepared by an organometallic process.

The crystal structure and lattice parameters were determined by x-ray diffraction. All compositions were orthorhombic Pbnm.

Pellets were pressed from powders of each composition and sintered to high density in a reducing atmosphere. When a small amount of Fe was substituted for Cr, the powder could be sintered in air.

Electrical conductivity for acceptor doped $NdCrO_3$ varied from about 1 $(ohm\ cm)^{-1}$ at room temperature to about 10 $(ohm\ cm)^{-1}$ at 900°C, about two orders of magnitude higher than the electrical conductivity of the undoped $NdCrO_3$. The activation energy for conduction was lowered by acceptor doping (from 0.18 to 0.08 ev).

The thermal expansion coefficient of $NdCrO_3$ was 7.5 X 10^{-6}/°C. Doped and Al substituted material had higher thermal expansion coefficients, with no crystallographic transitions being observed in any composition with thermal expansion measurements to 900°C.

ACKNOWLEDGEMENT

The author would like to thank Dr. Harlan U. Anderson, his academic advisor, for helpful discussions and guidance during the course of this work.

Thanks to Beth Lenhart for assistance with Russian literature, and to Dean Anderson for making some of the thermal expansion measurements.

TABLE OF CONTENTS

LIST OF ILLUSTRATIONS

LIST OF TABLES

I. INTRODUCTION

During the last decade there has been an increasing need for more energy efficient methods of electrical power generation. As a result, generation of electrical power by means of magnetohydrodynamic (MHD) power generators has and is being seriously considered. An open cycle MHD generator operates at a much higher temperature than a steam turbine, so the efficiency of the MHD plant has the potential to be much higher than that of a conventional power plant.

In addition, coal, our most abundant fuel can be used as the source of the plasma without creating a serious air pollution problem. If potassium is added to the flame, it will combine with the sulfur from the coal to form K_2SO_4. Thus, the sulfur oxides from high sulfur coal are not released into the atmosphere.

The principles of MHD are well understood. A conducting gas, produced by burning coal and seeding the flame with potassium to increase the conductivity, flows through a channel with a velocity V. Perpendicular to the flow a strong magnetic field B is produced by a superconducting magnet. Perpendicular to both, an electric field $E = B \times V$ causes a current to flow through the load, which is connected to electrodes in the walls of the channel.

Eventhough the theory is simple, the engineering problems that must be solved before MHD can be economical are tremendous. One of the greatest problems is the lack of a suitable electrode material. Electrodes can be made using water cooled metal, but heat losses due to the cooling reduce efficiency slightly (Robinson, 1969). Ceramic electrodes can operate at higher temperatures, so overall plant

efficiency is ½ to 1% higher (Meadowcroft, 1969).

The requirements for electrodes, given by Yerouchalmi et. al. (1966) are difficult to meet with any material. The electrodes must withstand gas temperatures of 2500°C and resist chemical corrosion, ablation, and erosion with gas velocities of 700-800m/sec. Thermal cycling and the presence of high temperature gradients requires good thermal shock capabilities. In addition to chemical stability, the electrodes must also resist electrochemical corrosion and polarization. If they cannot survive longer than 1,000 hours in this severe environment, down time will be great and maintenance costs will be high so long term stability is important. To prevent joule heating losses the electrode conductivity at the power leadout must be at least 50-100 mho/cm, and for good current transfer it must be a good electron emitter at the plasma interface.

Neodymium chromite is one of a group of rare earth chromites with a distorted perovskite structure which are being considered for use as MHD electrodes. These oxides have high melting points, good chemical corrosion resistance, and high electrical conductivity. However, they are not very resistive to attack by coal slag when current densities exceed 1-2 amps/cm^2 (Cadoff et. al. 1977).

Zirconia appears to be quite resistive to electrochemical corrosion, but unfortunately it decomposes at high current densities due to the polarization which results from its ionic conductivity (Cadoff et. al. 1977).

Thus it appears that no oxide by itself will be suitable for use as an electrode in a coal fired MHD generator. As a result, Keler (1976) proposed that a composite electrode be used. A thin layer of stabilized zirconia would be on the inside of the MHD channel, in contact with the hot gases. Zirconia has good properties at high temperatures, but below 1400°C its conductivity is too low. A layer of $NdCrO_3$ would be used as a current leadout to carry the electric current from the zirconia layer to a metal conductor at 300-400°C or less. The resistivity of calcium doped $NdCrO_3$ is reported as 0.25 ohm-cm at 1300°C and 5 ohm-cm at room temperature, and the material has good chemical compatibility with stabilized zirconia to 1650°C. Keler (1976) also reports that $NdCrO_3$ could be air fired, fired in a reducing atmosphere, or hot pressed so a composite of the two materials is possible. Thus an electrode would result which might be suitable for MHD electrode applications.

Since very little information is available regarding the influence of dopants on electrical conductivity, thermal expansion, and fabrication of $NdCrO_3$ based compositions, except that reported by Keler, a more thorough study must be made so that this material can be properly evaluated. For example, it is known that the coefficient of thermal expansion of $NdCrO_3$ is too low to allow direct contact with ZrO_2 (7.4×10^{-6} compared to $10.5 \times 10^{-6} {}^{o}C^{-1}$). Thus if such a composite structure is to be made, the coefficient of thermal expansion must be adjusted to match that of ZrO_2. It was the intent of this investigation to generate some of the required information. This was done by measuring lattice parameters, electrical

conductivity, and thermal expansion coefficients as functions of Al, Mg, and Ca content and temperature. The influence of oxygen activity on densification and microstructure was also investigated.

II. LITERATURE REVIEW

A. CRYSTAL STRUCTURE

Keith and Roy (1954) made $NdCrO_3$ and $NdAlO_3$ by mixing and heating fine oxide powders. Powder diffraction studies indicated that the compounds had distorted perovskite structures, but because of the fine particle size and the similarities of the x-ray patterns of the various structures, they had difficulty determining what type of distorted perovskite structure was present in each compound. They reported that $NdCrO_3$ was rhombohedral or monoclinic distorted perovskite structure, and that $NdAlO_3$ was rhombohedral.

Remeika (1956) grew single crystals of rare earth compounds using PbO as a flux for most of the compounds, and Bi_2O_3 for the chromites. His $GdFeO_3$ single crystals were used by Geller (1956) for determination of the crystal structure. There are four distorted perovskite units in the orthorhombic cell, and the space group is Pbnm. Geller (1957) then made a powder diffraction study which included $NdCrO_3$. He found that $NaCrO_3$ is isostructural with $GdFeO_3$. (Lattice parameters given in Table I.) Geller and Bala (1956) made a powder diffraction study of rare earth aluminates and found that $NdAlO_3$ is rhombohedral with $\underline{a}$ = 5.286Å and $\alpha = 60°25'$. For similar compounds high temperature x-ray and optical studies showed orthorhombic to rhombohedral and rhombohedral to cubic transformations, but no high temperature measurements were made on Nd compounds.

Wold and Croft (1959) found complete solid solution between $NdCrO_3$ and $NdFeO_3$ with orthorhombic Pbnm structure over the entire

TABLE I.

REPORTED LATTICE PARAMETERS FOR $NdCrO_3$

Investigator(s)	a (Å)	b (Å)	c (Å)
Geller (1957)	5.412	5.494	7.695
Wold and Croft (1957)	5.411	5.471	7.702
Quezel-Ambrunaz and Mareschal (1963)	5.425	5.478	7.694

range of compositions. The lattice parameters of $NdFeO_3$ were a = 5.456Å, b = 5.585Å, and c = 7.761Å; and the values for $NdCrO_3$ are listed in Table I.

B. PHASE EQUILIBRIA

Schneider, Roth, and Waring (1961) found only one compound, $NdCrO_3$, in the system Nd_2O_3-Cr_2O_3. In the system Nd_2O_3-Al_2O_3 the only compound was $NdAlO_3$. No transformations were observed upon heating either system. They also made a plot of various ABO_3 compounds in which the radius of the A ion was on one axis and the radius of the B ion was on the other. This plot showed the regions of stability of the various crystal structures as a function of ionic size. Neodymium chromite was found to be near the middle of the orthorhombic region and $NdAlO_3$ just over the boundary, inside the rhombohedral region.

Figure 1 is the phase diagram for the system Cr_2O_3-Nd_2O_3 determined by Pavlikov and Tresvyatskii (1966). They again found $NdCrO_3$ to be the only compound.

Toropov and Kiseleva (1961) gave the phase diagram for the system Nd_2O_3-Cr_2O_3, and found a eutectic between $NdCrO_3$ and Cr_2O_3 at 22 mole percent Nd_2O_3, 78 mole percent Cr_2O_3, and 2080 $\pm$ 30°C. The only compound is $NdCrO_3$, melting at 2330 $\pm$ 30°C. (Figure 2)

Zyrin, Dubok, and Tresvyatskii (1965) determined the melting points of several materials by contact-free heating in a resistance furnace. Neodymium chromite and $NdAlO_3$ melted at 2420°C and 2070°C respectively.

Foex (1968) used high-temperature x-ray analysis to determine

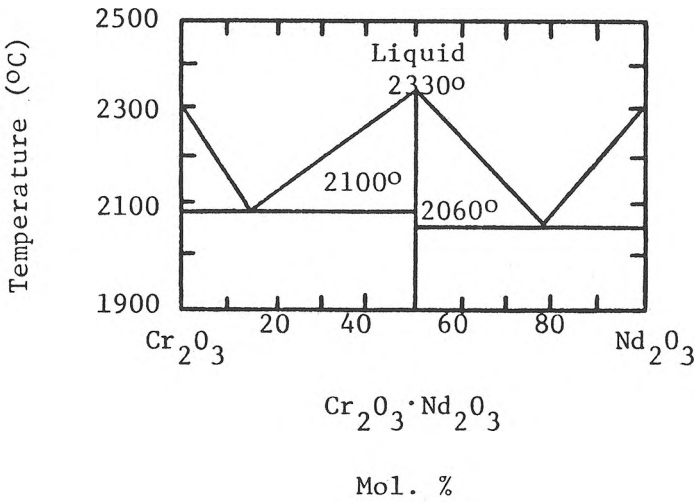

FIGURE 1. THE SYSTEM Cr_2O_3-Nd_2O_3

(Pavlikov and Tresvyatskii, 1966)

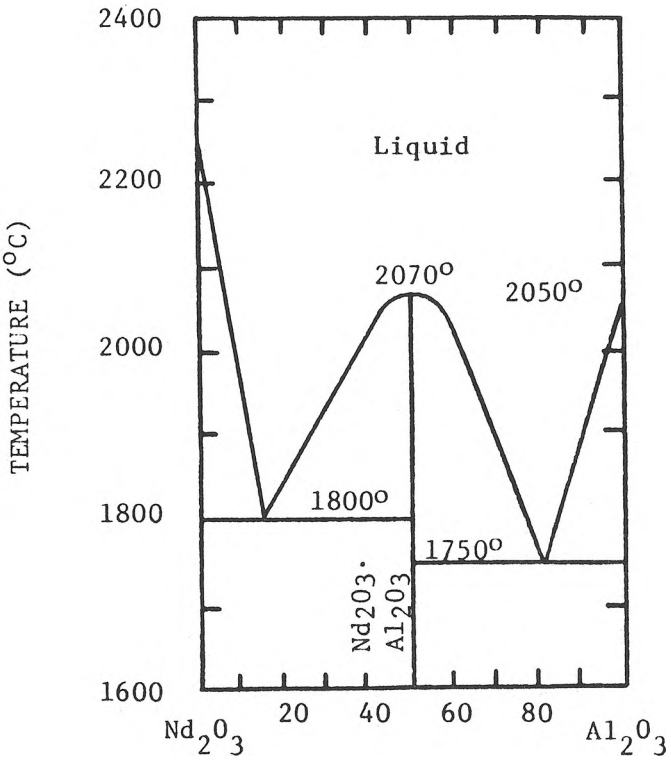

FIGURE 2. THE SYSTEM Al_2O_3-Nd_2O_3

(Toropov and Kiseleva, 1961)

solidification points. Neodymium chromite and $NdAlO_3$ solidified at 2405°C and 2090°C respectively.

Using a solar furnace, Coutures, Berjoan, and Granier (1973) found that $NdCrO_3$ melts at 2350-45°C in oxygen, and at 2410 $\pm$ 5°C in argon.

Keler (1976) reported that $NdCrO_3$ will not react with a solid solution of ZrO_2-Y_2O_3-Nd_2O_3 to 1650°C, and that it can be sintered in air at 1700-1750°C, or sintered in a vacuum or hot pressed so that the ZrO_2 solid solution can be sintered along with it.

Strakhov, Gorbunova, Nivokov, and Sergeev (1976) studied the reaction kinetics of the system Nd_2O_3-MgO-Cr_2O_3. Above 1200°C, only $NdCrO_3$ formed. Some $MgCr_2O_4$ formed at lower temperatures, but when it was heated, it decomposed to form $NdCrO_3$. In mixtures of the system Nd_2O_3-MgO-Al_2O_3, they found that $MgAl_2O_4$ formed more rapidly than $NdAlO_3$ at low temperatures, but above 1400°C $MgAl_2O_4$ decomposed to form $NdAlO_3$. At high temperatures, neither $NgCr_2O_4$ nor $MgAl_2O_4$ was stable in the presence of Nd_2O_3. $NdCrO_3$ and $NdAlO_3$ were the stable phases in the two systems.

C. DENSITY

Portnoi and Timofeeva (1965) reported pyconometer densities of 6.95g/cm^3 for $NdCrO_3$ and 6.7g/cm^3 for $NdAlO_3$. They used powder with a particle size less than one micron and toluene in their experiments.

Geller (1957) found an x-ray density of 7.09g/cm^3 for $NdCrO_3$, and Geller (1956) also reported an x-ray density of 6.91g/cm^3 for $NdAlO_3$.

D. ELECTRICAL CONDUCTIVITY

Zyrin, Dubok, and Tresvyatskii (1965) studied $Nd_{1-x}Sr_xCrO_3$ where x equals 0, 0.1, 0.2, 0.4, and 0.8. In the graph of log resistivity as a function of 1/T, there were two linear portions with a break near 380-420°C. They concluded that the room temperature conductivity was proportional to the dopant concentration, and that the mobility did not vary with dopant concentration. They attempted to make Hall effect measurements, but the the mobility was too low for measurements to be made. Calcium doped specimens were also tested, and they had slightly higher conductivity than specimens doped with the same amount of Sr. The thermoelectric emf coefficient was positive and increased with increasing temperature, except for the pure $NdCrO_3$ where it first decreased, then increased, with a minimum at 380-400°C. The sign of the thermoelectric emf coefficient indicated hole conduction. It was claimed that "insertion of divalent ions in the chromite crystal leads to the same amount of (hole) carrier current." The mobility was calculated from the electrical conductivity by assuming that the number of carriers was equal to the number of divalent ions added to the crystal, and it was stated that "The increase in electrical conductivity with rise in temperature can be ascribed to the increase of carrier mobility, but not to an increase in carrier concentration." The low temperature electrical conduction, where activation energy was higher, was attributed to polaron scattering, and conduction at high temperatures, with lower activation energy, was attributed to a hopping model.

Anthony and Foex (1966) gave a conductivity of 40 mho/m at 1400°C for undoped $NdCrO_3$.

Gordon et. al. (1971) made four-probe measurements of the conductivity of rare earth chromites at high temperatures, and at pressures of 10^{-2} to 10^{-3} torr. The activation energy was 0.8 ev for $NdCrO_3$, with a break in the curve at 1720 $\pm$ 20°C which was attributed to a transition to intrinsic conductivity.

Keler (1976) reported resistivities of 5 ohm cm at room temperature and 0.25 ohm cm at 1300°C for Ca doped $NdCrO_3$.

E. THERMAL EXPANSION

Henry and Thompson (1976) reported the thermal expansion coefficient of $NdCrO_3$ to be $7.89 \times 10^{-2}/°C$ from 25 to 500°C, $8.31 \times 10^{-6}/°C$ from 25 to 1000°C, and $8.60 \times 10^{-6}/°C$ from 25 to 1200°C. Neodymium Aluminate has thermal expansion coefficients of $10.1 \times 10^{-6}/°C$ from 25 to 500°C, $10.7 \times 10^{-6}/°C$ from 25 to 1000°C, and $10.9 \times 10^{-6}/°C$ from 25 to 1200°C.

Pavlikov, Lopato, and Tresvyatskii (1966) measured the thermal expansion of several rare earth chromites. Lanthanum chromite showed a transition from orthorhombic to rhombohedral with a decrease in length at 20 $\pm$ 5°C, but for the other chromites, including $NaCrO_3$, there was no transition from 25°C to 900°C. The average thermal expansion coefficient of $NdCrO_3$ from 25°C to 900°C was $8.3 \times 10^{-6}/°C$.

F. HARDNESS

Portnoi and Timofeeva (1965) found a microhardness of

1600-1700 kg/mm^2 for fused $NaCrO_3$.

III. EXPERIMENTAL PROCEDURE

A. FABRICATION

The raw materials, their sources, and, where available, the chemical analyses given by the manufacturers, are listed in Table II. The Nd_2O_3 was put into solution by dissolving it in about 1.5 ml concentrated HNO_3, 3-4 grams of citric acid, and about 8 ml of ethylene glycol for each gram of oxide. The solution was heated gently on a hot plate under a hood. At about 85°C, the hot plate was turned off. The hot plate still heated the beaker to 90°C, and at this temperature there was an exothermic reaction which heated the solution rapidly to about 110°C. At this temperature nitrate fumes boiled off violently. After boil off, a stable organic solution remained.

The solution and the solid raw materials were analyzed by decomposing known amounts at 1000°C overnight to drive off CO_2, H_2O, nitrates, and other volatile materials. The remaining powder was weighed, and the weight fraction of oxide in the raw materials was calculated by assuming that all of the remaining material was pure oxide.

A 25 gram batch of each composition listed in Table III was made by the method developed by Pechini (1967). The proper amounts of the solid raw materials were weighed out and dissolved in water using nitric acid. They were mixed with the neodymium solution, and the resulting solution was heated to drive off the nitrates, the water, and some of the organic material. When the material was

TABLE II

RAW MATERIALS

Calcium Carbonate, Fisher Certified

Typical Cation Analysis (by wt.)

Insoluble in dilute HCl	0.01 %
Ba	0.005%
Heavy Metals (such as Pb)	0.001%
Fe	0.002%
Mg	0.02 %
K	0.01 %
Na	0.1 %
Sr	0.1 %

Chromium Nitrate, Fisher Certified

Typical Impurity Analysis (by wt.)

Alkali Salts	0.05 %
Cl	0.002%
Fe	0.005%
SO_4	0.005%

Aluminum Nitrate, Matheson, Coleman and Bell,

98% minimum, Typical Analysis (by wt.)

Cl	0.001%
Heavy Metals (such as Pb)	0.001%

TABLE II (Continued)

Insoluble Material	0.005%
Fe	0.002%
SO_4	0.005%
Substances not precipitated by NH_4OH	0.05 %

Iron Nitrate, Fisher Certified

Typical Analysis (by wt.)

Insoluble Material	0.005%
Cl	5 ppm
SO_4	0.01 %
Substances not precipitated by NH_4OH	0.1 %

Magnesium Carbonate, Fisher Certified

Typical Analysis (by wt.)

Insoluble in HCl	0.015%
Cl	0.010%
NO_3	0.003%
Ba	0.005%
Ca	0.2 %
Zn	0.01 %
Heavy metal (such as Pb)	0.002%
SO_4	0.02 %
Water soluble substances	0.40 %

TABLE II (Continued)

Neodymium Oxide, Apache Chemical

99.9% purity (to other rare earths) (by wt.)

TABLE III.

NOMINAL COMPOSITIONS PREPARED

$NdCrO_3$

$Nd_{.95}Ca_{.05}CrO_3$

$Nd_{.9}Ca_{.1}CrO_3$

$Nd_{.8}Ca_{.2}CrO_3$

$NdCr_{.98}Mg_{.02}O_3$

$NdCr_{.95}Mg_{.05}O_3$

$NdCr_{.9}Mg_{.1}O_3$

$Nd_{.95}Ca_{.05}Cr_{.9}Al_{.1}O_3$

$Nd_{.95}Ca_{.05}Cr_{.8}Al_{.2}O_3$

$Nd_{.95}Ca_{.05}Cr_{.5}Al_{.5}O_3$

$Nd_{.95}Ca_{.05}Cr_{.95}Fe_{.05}O_3$

charred, it was transferred to a crucible and calcined at 750°C for several hours to burn off the remaining organic material and form a very fine powder of the desired composition.

An attempt was made to synthesize some of the compositions from solid Nd_2O_3 instead of the Nd solution. The Nd_2O_3 could be dissolved in HNO_3, but after the other raw materials were added, it tended to come out of solution and would not react with the other raw materials to form the desired compounds.

The resulting powder was prepared for compaction by the addition of ten to twelve weight percent PVA and water solution. The powder plus binder was mixed and then forced through a 40 mesh plastic screen to break up clumps and to distribute the binder more evenly. After pressing at 20,000 psi the green strength of the pressed parts was high enough so that they could be cut with a sharp knife and drilled with a diamond drill. One composition was compacted using 5% distilled water instead of PVA and water binder. This material pressed well and sintered to a high density, but the green strength was lower.

The pellets were sintered at 1750°C for 90 minutes in various O_2 partial pressures. Mixtures of CO_2 and H_2 were used to achieve the desired oxygen partial pressures. The O_2 partial pressures were measured with a zirconia cell and temperature was measured with an optical pyrometer. Pellets that were sintered at less than ambient O_2 pressure were annealed in air at 1400°C for 24 hours.

B. X-RAY DIFFRACTION

X-ray analysis on sintered compacts and powders was made using a General Electric XRD-700 diffractometer and Cu K_α radiation. Diffraction patterns from dense, sintered compacts gave more intense and sharper lines than the corresponding powders. However, due to the lack of an internal standard and alignment problems pellets were not used to determine lattice parameters. All lattice parameter measurements were made on powders which had been annealed at 1400°C for 24 hours.

The d spacings of the allowed reflections were calculated by computer using Geller's lattice parameters and the formula $1/d^2 = h^2/a^2 + k^2/b^2 + l^2/c^2$. The fast scans were indexed by comparing them to the calculated d spacings. There were several weak peaks due to $Nd(OH)_3$, but the others all matched with the calculated values.

Annealed powder of each composition was mixed with a NaCl internal standard. Slow scans were done at 0.2° per minute over the 111, 021, 022, 202, and 113 peaks. All the other peaks visible below 70° were due to multiple reflections. On some compositions, it was not possible to resolve the 022 peak from the 202 peak, so all lattice parameters were calculated from the 111, 021, and 113 peaks.

C. DENSITY

Density of the sintered pellets was determined by Archimedes' Principle in xylene. A $SrTiO_3$ single crystal was used to determine

the density of xylene. For the porous specimens, dry, saturated, and suspended weights were measured, but most specimens had no open porosity.

D. MICROSTRUCTURE

Sintered pellets of several compositions were ground and polished, then thermally etched at 1650°C for about 30 minutes. They were photographed on a Zeiss Axiomat at 1000x with oil immersion. Using the Nomarsky phase contrast mode more than one phase was observed in the $NdCrO_3$ and Ca doped $NdCrO_3$ fired with $P_{O_2} = 6 \times 10^{-12}$ atm. Three or four unknown phases were present in the $Nd_{.8}Ca_{.2}CrO_3$. When these compositions were fired with $P_{O_2} = 6 \times 10^{-11}$ atm, they were single phase.

E. ELECTRICAL CONDUCTIVITY

Prior to sintering, compacts were cut into bars about 1 inch long, 1/2 inch wide, and 1/16 inch thick. Four holes were drilled along the length of each bar. These specimens were sintered and used for electrical conductivity measurements. Annealing was especially important here since the conductivity was several orders of magnitude higher after annealing than before. For the first set of specimens, a Pt wire was simply placed in each hole and twisted to hold it in place. Four terminal measurements were made from room temperature to 900°C. For each measurement, the furnace was allowed to control for about ten minutes so that the specimen and the thermocouple would be at the same temperature. Temperature was measured with a chromel-alumel thermocouple and

a potentiometer or a digital volt meter. Resistance was measured with a Dana Model 5100 digital multimeter.

With some of the specimens, it was impossible to get low resistance connections simply by twisting the Pt wires onto the bar, so the specimens were masked except where the wires were to be attached, and then sputtered with Pt. After sputtering, the wires could attached by twisting and the resistance measured as before.

F. THERMAL EXPANSION

Bars of sintered material were placed inside a fused silica holder in a furnace. They were heated from room temperature to 900°C in steps of about 100°C. The furnace was allowed to control for a few minutes at each step then readings were taken. The change in length was measured with a LVDT and recorded with a Heath strip chart recorder. Temperature was measured with a thermocouple and a potentiometer or digital volt meter.

IV. RESULTS AND DISCUSSION

A. X-RAY DIFFRACTION

Several peaks due to $Nd(OH)_3$ were observed in all the x-ray patterns. When the specimens contained any excess Nd_2O_3, it reacted with moisture from the air to form $Nd(OH)_3$. Some specimens were initially made with a large excess of Nd_2O_3, and when the $Nd(OH)_3$ formed, the volume increase caused the sintered specimens to crumble to a fine powder. Evidently the amount of free Nd_2O_3 in the second batch of these compositions was not enough to destroy the sintered pellets, since after six months, no evidence of crumbling or degradation was visible. For these specimens the x-ray peaks due to $Nd(OH)_3$ were much weaker than in the batches that disintegrated. In these compositions, the slight Nd excess probably was due either to Cr vaporization during annealing and sintering, or error in the gravimetric analyses of the starting chemicals. Neither the lattice parameters nor the electrical conductivity were influenced by this reduction in the amount of free $Nd(OH)_3$, so the remaining amount was not judged to be significant and no attempt was made to eliminate it completely. The x-ray patterns determined for each composition are listed in Appendix A.

Table IV gives the lattice parameters determined in this study, and those determined by Geller (1957) and Quezel-Ambrunaz and Mareschal (1963) for comparison. The values of the lattice parameters and the limits of error in Table IV were determined from the slow scans by a method described in Appendix B. Geller's values for b and c were within the error limits, as were all of the lattice parameters

TABLE IV

LATTICE PARAMETERS, CELL VOLUME AND X-RAY DENSITY

Composition	a(Å)	b(Å)	c(Å)	V(Å^3)	D(g/cm^3)
	(1)	(2)	(3)		
$NdCrO_3$	5.419	5.492	7.690	228.9	7.086
$Nd_{.95}Ca_{.05}CrO_3$	5.413	5.482	7.680	227.9	6.965
$Nd_{.9}Ca_{.1}CrO_3$	5.410	5.470	7.674	227.1	6.838
$Nd_{.8}Ca_{.2}CrO_3$	5.401	5.450	7.647	225.1	6.591
$NdCr_{.98}Mg_{.02}O_3$	5.416	5.494	7.696	229.0	7.067
$NdCr_{.95}Mg_{.05}O_3$	5.412	5.494	7.695	228.8	7.049
$NdCr_{.9}Mg_{.1}O_3$	5.418	5.491	7.696	229.0	7.003
$Nd_{.95}Ca_{.05}Cr_{.9}Al_{.1}O_3$	5.418	5.454	7.652	226.1	6.947
$Nd_{.95}Ca_{.05}Cr_{.8}Al_{.2}O_3$	5.403	5.435	7.639	224.3	6.929
$Nd_{.95}Ca_{.05}Cr_{.5}Al_{.5}O_3$	5.395	5.363	7.591	219.6	6.851
$Nd_{.95}Ca_{.05}Cr_{.95}Fe_{.05}O_3$	5.430	5.478	7.660	227.9	6.971
$NdCrO_3$ (Geller)	5.412	5.494	7.695	228.8	7.09
$NdCrO_3$ (Quezel-Ambrunaz and Mareschal)	5.425	5.478	7.694	228.7	

1) 95% Confidence Limit = $\pm$ 0.005Å

2) 95% Confidence Limit = $\pm$ 0.002Å

3) 95% Confidence Limit = $\pm$ 0.005Å

of Quezel-Ambrunaz and Mareschal. The results of this study are in good agreement with the data from the literature.

Figures 3, 4 and 5 show the measured lattice parameters as functions of Ca, Mg and Al content respectively. As can be seen in Figures 3 and 5, the lattice parameters decrease with increasing Ca and Al content, whereas the lattice parameters show no dependence on Mg content in Figure 4.

The true values of the lattice parameters could lie anywhere between the minimum and maximum values calculated from the edges of the x-ray peaks in Appendix B, which were used to find the error limits in Table IV. Thus the error limits estimate the accuracy of the lattice parameter determinations. In order to estimate the precision of the lattice parameter determinations, s^2 was calculated as described in Appendix B for the lattice parameter values of the Mg doped specimens. The lattice parameters changed little with Mg content, so all the lattice parameter determinations were assumed to estimate the same set of lattice parameters and the s^2 values for a, b and c given in Table V estimate the variance of the determinations.

The lattice parameters decreased in a linear fashion with Ca content, so $s^2_{y.x}$ was calculated as shown in Appendix B to estimate the variance of the determinations of lattice parameters as a function of Ca content from a straight line. This gives another estimate of the precision of the determinations.

In order to get reproducible results, the lattice parameters of all the compositions were determined in the same manner. In Appendix B, 95% confidence intervals are calculated for a, b and c.

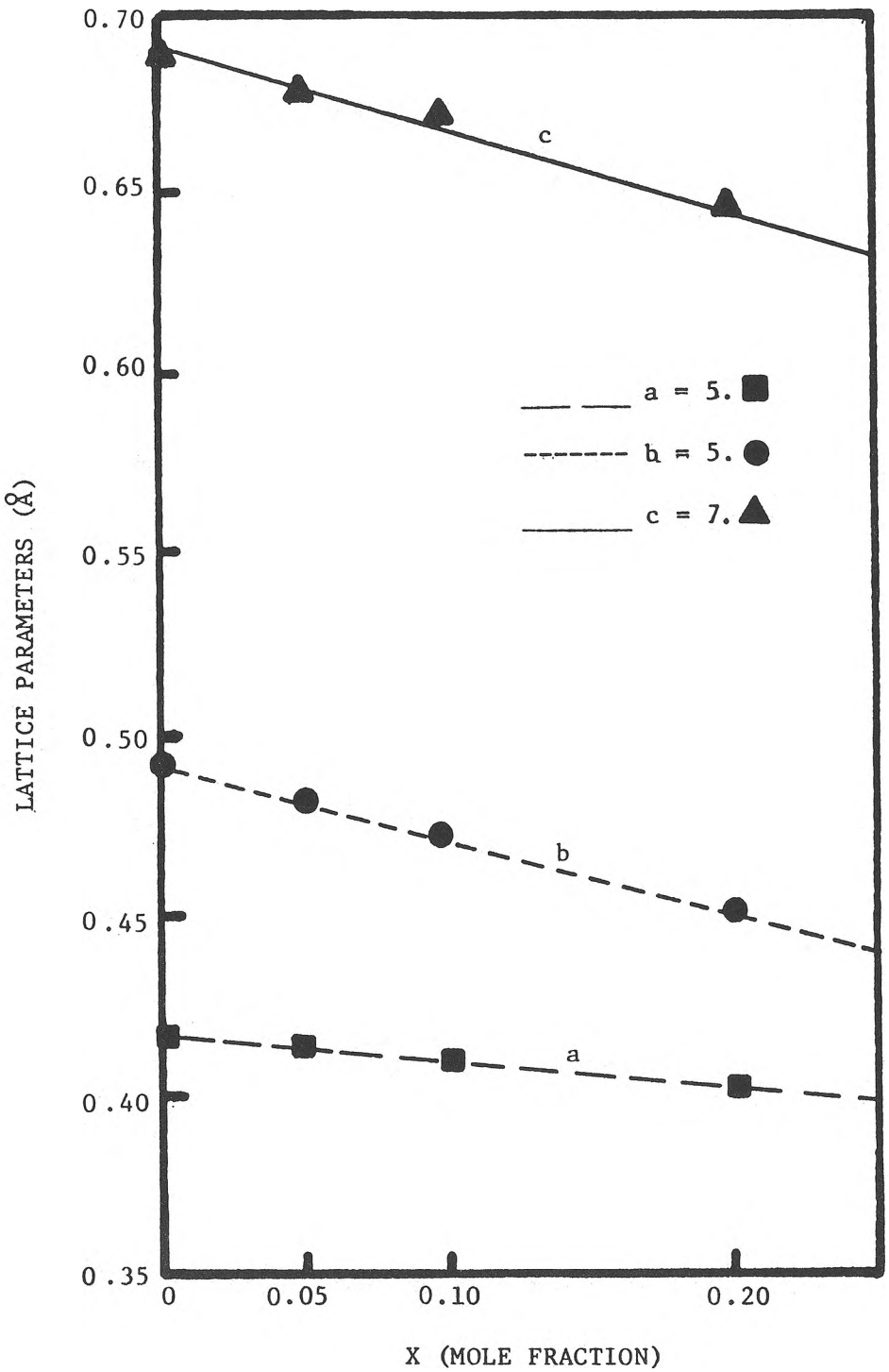

FIGURE 3. LATTICE PARAMETERS OF $Nd_{1-x}Ca_xCrO_3$

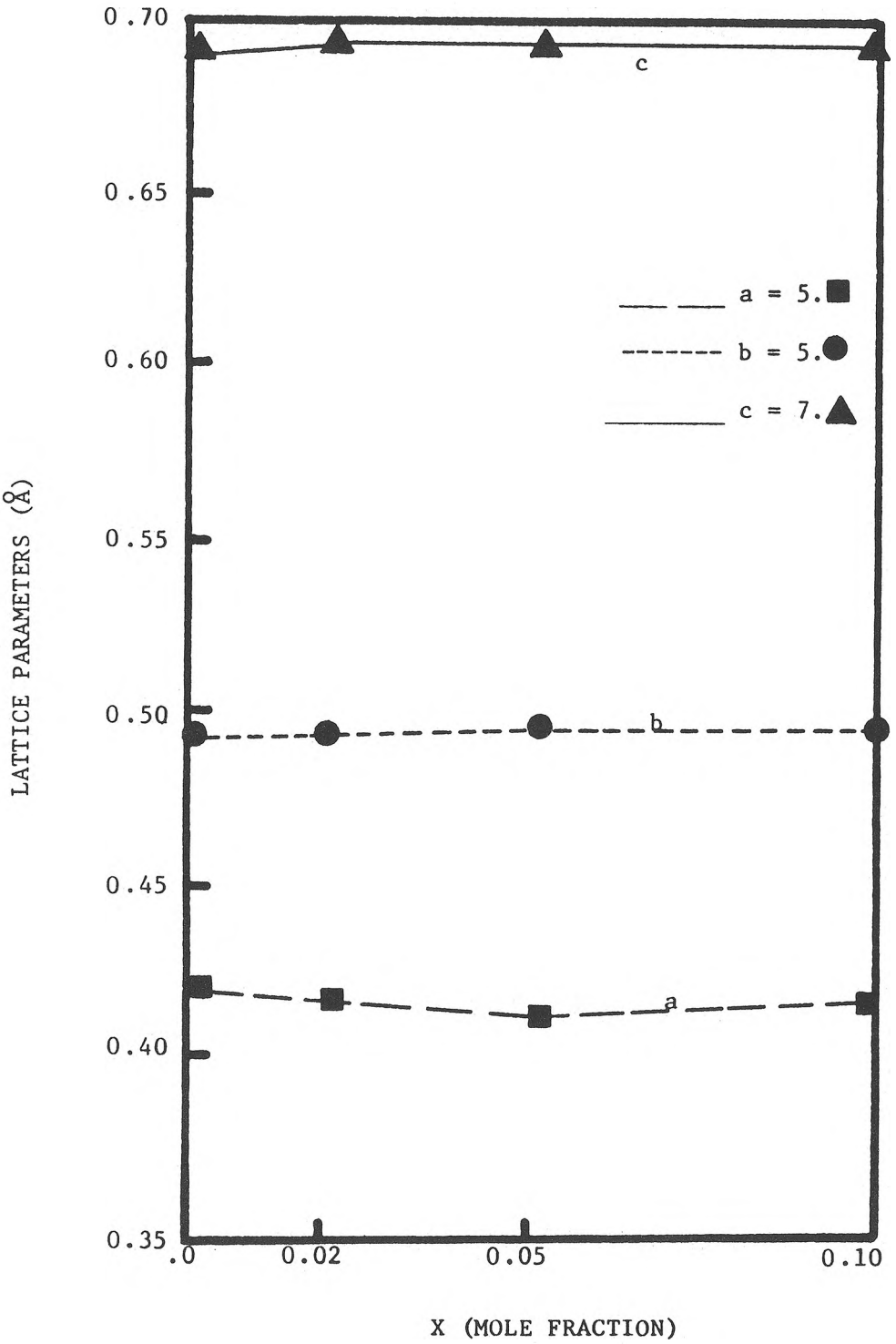

FIGURE 4. LATTICE PARAMETERS OF $NdCr_{1-x}Mg_xO_3$

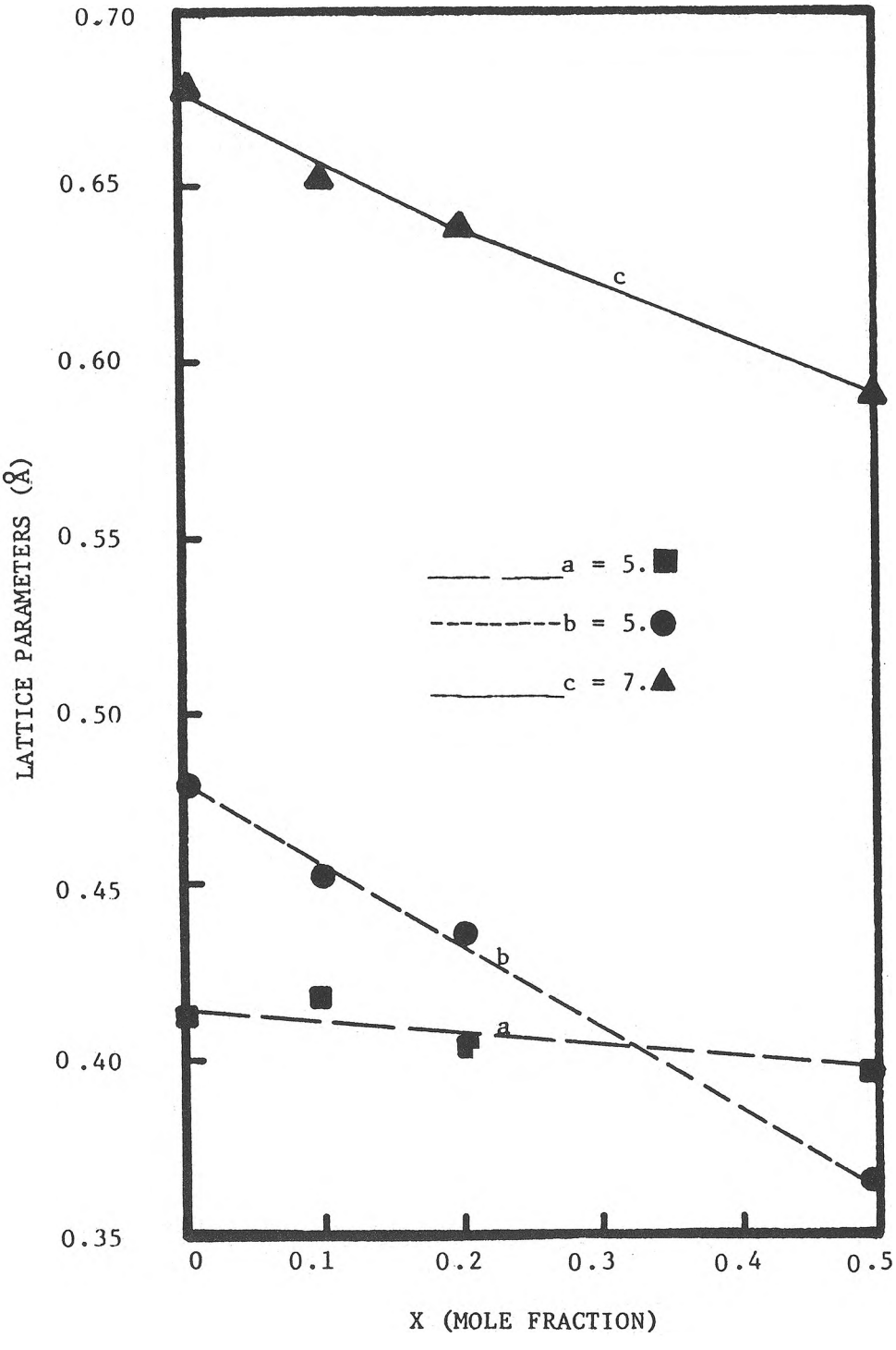

FIGURE 5. LATTICE PARAMETERS OF $Nd_{.95}Ca_{.05}Cr_{1-x}Al_xO_3$

TABLE V

VARIANCE OF LATTICE PARAMETERS

	a	b	c
Ca doped material			
$s^2_{y.x}$	7.71×10^{-7}	5.71×10^{-7}	1.05×10^{-5}
$s_{y.x}$	0.00088Å	0.00076Å	0.0032Å
Mg doped material			
s^2	9.58×10^{-6}	2.25×10^{-6}	8.25×10^{-6}
s	0.0031Å	0.0015Å	0.0029Å

95% confidence intervals for Mg doped material

$5.411\text{Å} < a < 5.421\text{Å}$ or $a = 5.416 \pm 0\text{-}005\text{Å}$

$5.491\text{Å} < b < 5.495\text{Å}$ or $b = 5.493 \pm 0.002\text{Å}$

$7.689\text{Å} < c < 7.699\text{Å}$ or $c = 7.694 \pm 0.005\text{Å}$

Non-statistical error limits for $NdCrO_3$

$5.415\text{Å} < a < 5.441\text{Å}$

$5.478\text{Å} < b < 5.495\text{Å}$

$7.678\text{Å} < c < 7.709\text{Å}$

These confidence intervals which are calculated from the s^2 values for Mg doped $NdCrO_3$ are given in Table V, and the length of these intervals is less than the length of the intervals between the maximum and minimum values calculated in Appendix B and presented in Table V. If the lattice parameter determinations are unbiased, and if, after making the measurement an infinite number of times the average of all the determinations would give the true lattice parameters then at the 95% level of confidence the true lattice parameters lie within the intervals. This means that 95% of the confidence intervals determined in this manner will contain the true lattice parameter (Stearman, 1955).

B. FABRICATION

The sintered densities of the compacts made in this study are given in Table VI. All pellets were densified at 1750°C for 90 minutes in various oxygen partial pressures. Only the iron doped specimen densified in air. The others were sintered close to theoretical density at 6×10^{-11} atm O_2. At 6×10^{-12} atm O_2, a second phase, probably chromium, formed. It can be seen in the microstructure in Figure 6. Density was not quite as high as at 6×10^{-11} atm O_2.

The sintering behavior was similar to that observed by Ownby and Jungquist (1972) for Cr_2O_3, and for several mixed oxides containing chromium, including $MgCr_2O_4$ (Anderson, 1978) and several orthochromites similar in structure to $NdCrO_3$. Chromium oxide densified best at 2×10^{-12} atm O_2 partial pressure. This is the equilibrium P_{O_2} for the reaction

$$2Cr + 3/2O_2 = Cr_2O_3$$

TABLE VI

SINTERED DENSITIES AND PERCENT OF X-RAY DENSITY ( )

Composition	Partial Pressure O_2 (atm) 0.2		6×10^{-11}		6×10^{-12}	
$NdCrO_3$	3.76g/cm^3	(53.0%)	6.31g/cm^3	(89.0%)	6.73g/cm^3	(95.0%)
$Nd_{.95}Ca_{.05}CrO_3$	3.96	(56.8%)	6.76	(97.0%)	6.41	(92.0%)
$Nd_{.9}Ca_{.1}CrO_3$	3.28	(47.9%)	6.20	(90.6%)	6.17	(90.2%)
$Nd_{.8}Ca_{.2}CrO_3$	3.65	(55.4%)	6.09	(92.3%)	6.23	(94.5%)
*$NdCr_{.98}Mg_{.02}O_3$	----	----	5.43	(76.8%)	----	----
*$NdCr_{.95}Mg_{.05}O_3$	----	----	4.45	(63.1%)	----	----
*$NdCr_{.9}Mg_{.1}O_3$	----	----	5.81	(82.9%)	----	----
*$Nd_{.95}Ca_{.05}Cr_{.9}Al_{.1}O_3$	----	----	5.49	(79.0%)	----	----
*$Nd_{.95}Ca_{.05}Cr_{.8}Al_{.2}O_3$	----	----	6.41	(92.5%)	----	----
*$Nd_{.95}Ca_{.05}Cr_{.5}Al_{.5}O_3$	----	----	6.66	(97.2%)	----	----
$Nd_{.95}Ca_{.05}Cr_{.95}Fe_{.05}O_3$	6.80	(97.6%)	----	----	----	----

*Powder calcined at 1400^{o}C prior to sintering.

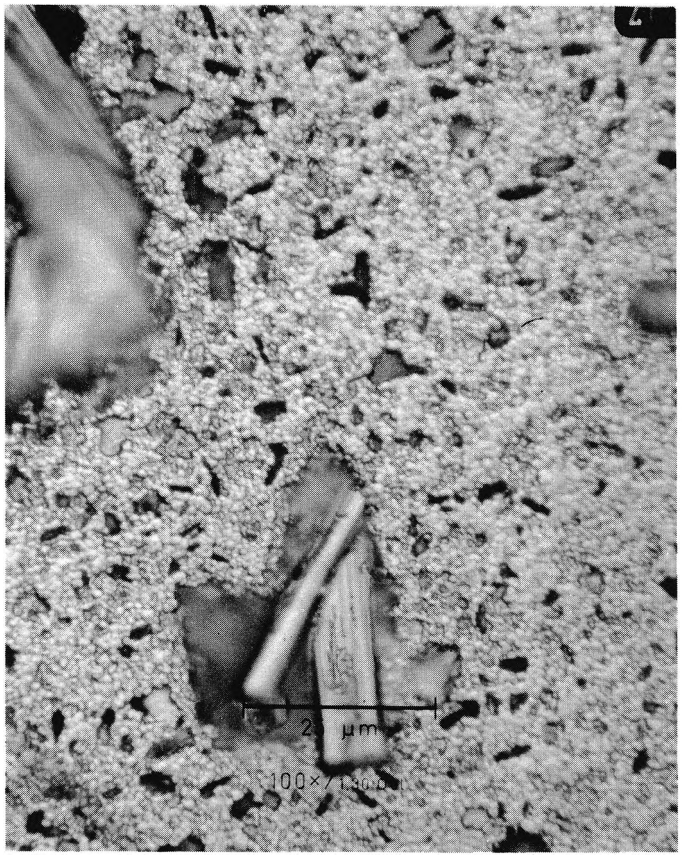

FIGURE 6. MICROSTRUCTURE OF $Nd_{.80}Ca_{.20}CrO_3$ SINTERED WITH 6 X 10^{-12} atm O_2 PARTIAL PRESSURE, T = 1750°C, 1,000X

When oxygen partial pressure was further reduced, the sintered densities were not as high. The dependence of sintering on oxygen pressure is attributed to changes in the oxidation state of Cr. Depending on P_{O_2}, Cr can exist in +6, +4, +3, +2, and valence states. The vapor pressures of all but the +3 state are high, so when the P_{O_2} is such that these other states exist, sintering occurs by evaporation and condensation. No densification occurs, but necks do grow between particles and particle size increases. At the equilibrium pressure for the +3 state, vapor phase transport is suppressed, so sintering is by volume diffusion, and the material densifies.

Ownby and Jungquist (1972) also found that the grain size was less in Cr_2O_3 doped with MgO than in pure Cr_2O_3. They found that the MgO segregated at the grain boundaries and formed $MgCr_2O_4$. In this study, exaggerated grain growth occured in the undoped $NdCrO_3$ sintered at $P_{O_2} = 10^{-11}$ atm.

In Figure 7, the grains have grown to about 20 microns. This rapid grain growth trapped pores inside the grains. These trapped pores cannot be eliminated, so the final density of the material is reduced. Also, the large pores and grain boundaries of this material lower the strength. Davidge (1979) shows that ceramics tend to have surface flaws extending one grain diameter, so coarse grained materials have larger flaws and break at lower stresses.

Calcium additions greatly reduce grain size. Figures 8, 9, and 10, show the fine grained materials produced with additions of calcium. The black spots in these microstructures are probably due to grain pull out during polishing, not porosity. The material with 5 percent Ca had

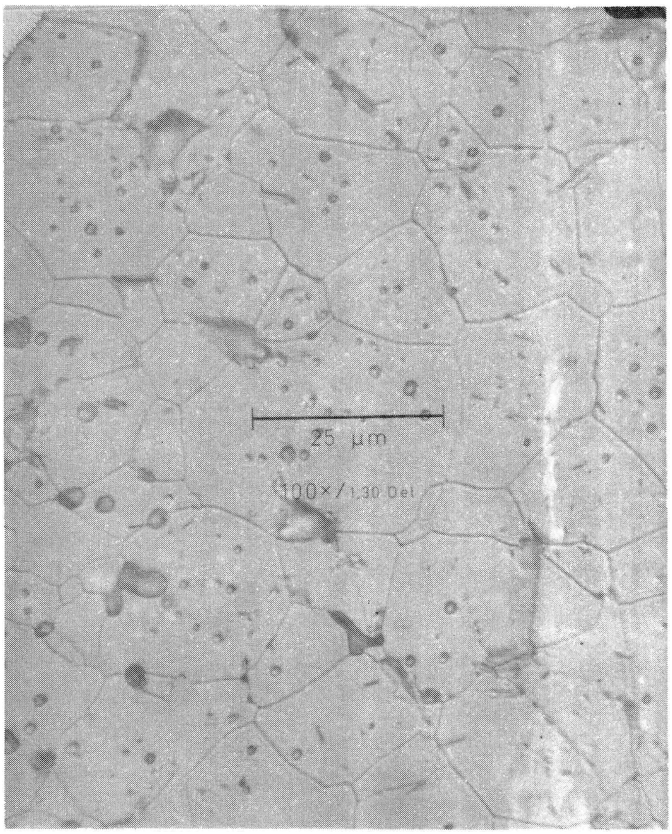

FIGURE 7. MICROSTRUCTURE OF $NdCrO_3$ SINTERED WITH 6 X 10^{-11} atm O_2 PARTIAL PRESSURE, T = 1750°C, 1,000X

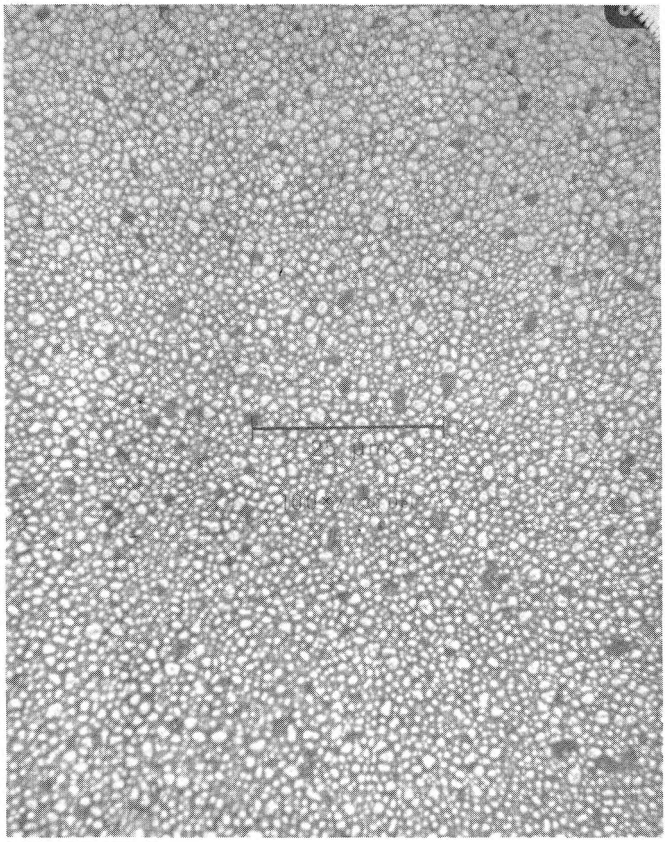

FIGURE 8. MICROSTRUCTURE OF $Nd_{.95}Ca_{.05}CrO_3$ SINTERED WITH 6 X 10^{-11} atm O_2 PARTIAL PRESSURE, T = 1750°C, 1,000X

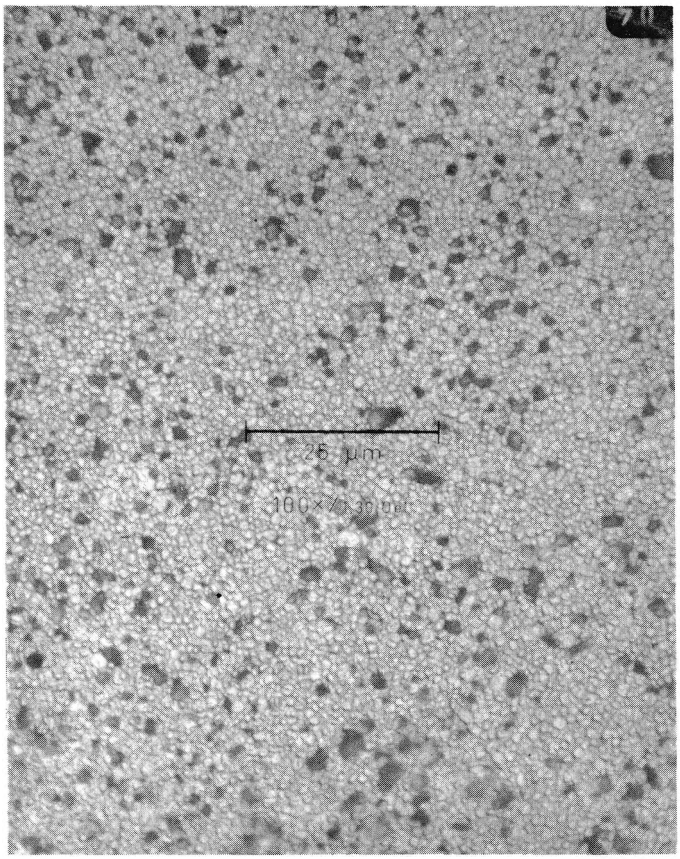

FIGURE 9. MICROSTRUCTURE OF $Nd_{.90}Ca_{.10}CrO_3$ SINTERED WITH 6 X 10^{-11} atm O_2 PARTIAL PRESSURE, T = 1750°C, 1,000X

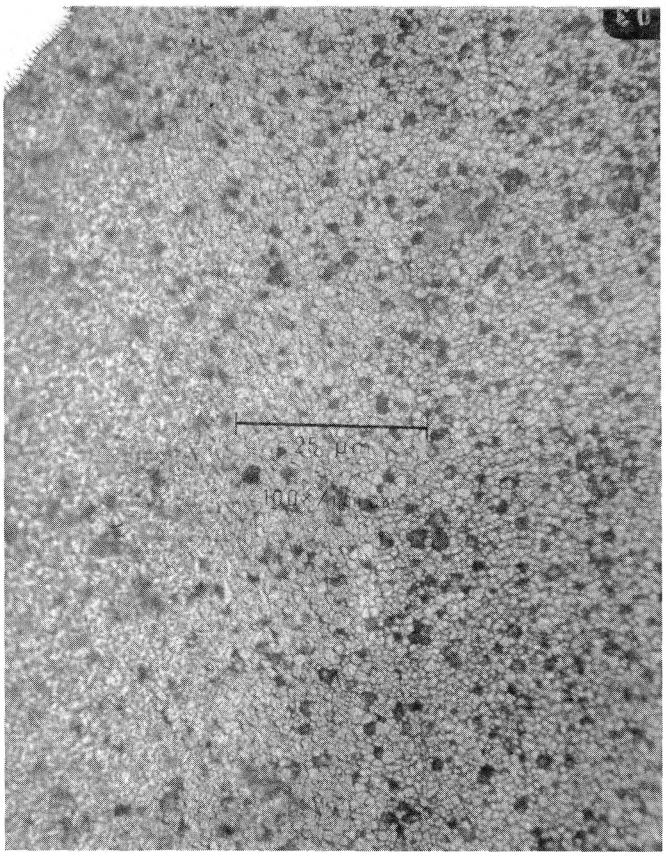

FIGURE 10. MICROSTRUCTURE OF $Nd_{.80}Ca_{.20}CrO_3$ SINTERED WITH 6 X 10^{-11} atm O_2 PARTIAL PRESSURE, T = 1750°C, 1,000X

the highest density and the least pull outs, so it probably had the highest strength.

The undoped $NdCrO_3$ and the Ca-containing compositions were only calcined to 750°C before sintering, but the Mg and Al containing specimens were annealed at 1400°C. The difference in density between these two groups of compositions (See Table VI) is probably due to increased initial grain size in the materials annealed at 1400°C. The 1400°C annealed specimen with the greatest density, $Nd_{.95}Ca_{.05}Cr_{.5}Al_{.5}O_3$ at 97.2% of theoretical density, was pressed with water instead of the PVA binder used with the other compositions. This probably increased the green density and yielded a denser sintered compact.

The Fe doped material was sintered close to theoretical density in air. This was probably due to the formation of a liquid phase. Keler (1976) said that $NdCrO_3$ could be sintered in air, and it is possible that the $NdCrO_3$ contained an iron impurity, perhaps from milling with steel balls.

C. ELECTRICAL CONDUCTIVITY

The conductivity of all the compositions followed the equation

$$\sigma = \sigma_o \exp(E_a/kT)$$

where σ is the conductivity, E_a is the activation energy for conduction, k is Boltzman's constant and T is the absolute temperature.

Table VI shows that the density of the sintered specimens varied from 97.6% of theoretical density for $Nd_{.95}Ca_{.05}Cr_{.95}Fe_{.05}O_3$ to 63.1% for $NdCr_{.95}Mg_{.05}O_3$. The differences in density were largely due to differences in the initial particle size of the powders. Porosity decreases the conductivity of the specimens. To describe the resistivity

of a two-phase material consisting of spheres in a matrix, Maxwell derived the equation

$$K = \frac{2k_1 + k_2 + p(k_1 - k_2)}{2k_1 + k_2 - 2p(k_1 - k_2)} k_2$$

where k_1 is the resistivity of dispersed spheres, k_2 is the resistivity of the matrix, p is the volume fraction of the spheres, and K is the resistivity of the matrix with the spheres. The volume fraction of spheres is assumed to be small so that there is no interaction between spheres. This is probably not a good assumption for the more porous specimens, but the equation holds for higher values of p when the resistivity of the dispersed phase, in this case pores, is much higher than the resistivity of the matrix. If the resistivity of the pores is very high,

$$K = \frac{2 + p}{2 - 2p} k_2.$$

This equation was used to correct the conductivity measurements of all the specimens for porosity.

The data were plotted on graphs of log conductivity vs. 1/T, and a line was fitted to the plot for each composition by the least squares method. The activation energy, E_a, determined from the slope of the line, and σ_o, determined from the intercept, are given in Table VII. The variance of the experimental points from the least squares line is given by $s^2_{\log \sigma.1/T}$, which is calculated in the same way as for the graphs of lattice parameter vs. Ca content in Appendix B. The number of data points taken for each composition is n in Table VII.

The conductivity data for $NdCrO_3$ and $Nd_{1-x}Ca_xCrO_3$ are plotted in Figure 11, along with data from the literature for comparison. The

TABLE VII

ELECTRICAL CONDUCTIVITY

Composition	σ_o $(ohm\ cm)^{-1}$	E_a (eV)	$s^2_{\log \sigma.1/T}$	n
$NdCrO_3$				
First Run	1.53	0.14	0.00507	6
Three Runs Combined	2.04	0.16	0.00927	13
$Nd_{.95}Ca_{.05}CrO_3$	23.6	0.087	0.000039	6
$Nd_{.9}Ca_{.1}CrO_3$	24.3	0.083	0.00299	6
$NdCr_{.98}Mg_{.02}O_3$	6.86	0.11	0.00257	4
$NdCr_{.95}Mg_{.05}O_3$	17.0	0.081	0.00283	5
$NdCr_{.9}Mg_{.1}O_3$	15.6	0.082	0.000517	5
$Nd_{.95}Ca_{.05}Cr_{.9}Al_{.1}O_3$	23.5	0.074	0.000305	6
$Nd_{.95}Ca_{.05}Cr_{.8}Al_{.2}O_3$	22.9	0.067	0.00129	6
$Nd_{.95}Ca_{.05}Cr_{.5}Al_{.5}O_3$	9.02	0.085	0.0123	6
$Nd_{.95}Ca_{.05}Cr_{.95}Fe_{.05}O_3$				
"Pure"	10.8	0.055	0.0698	10
Combined data, with and without impurity.	12.3	0.048	0.0508	14

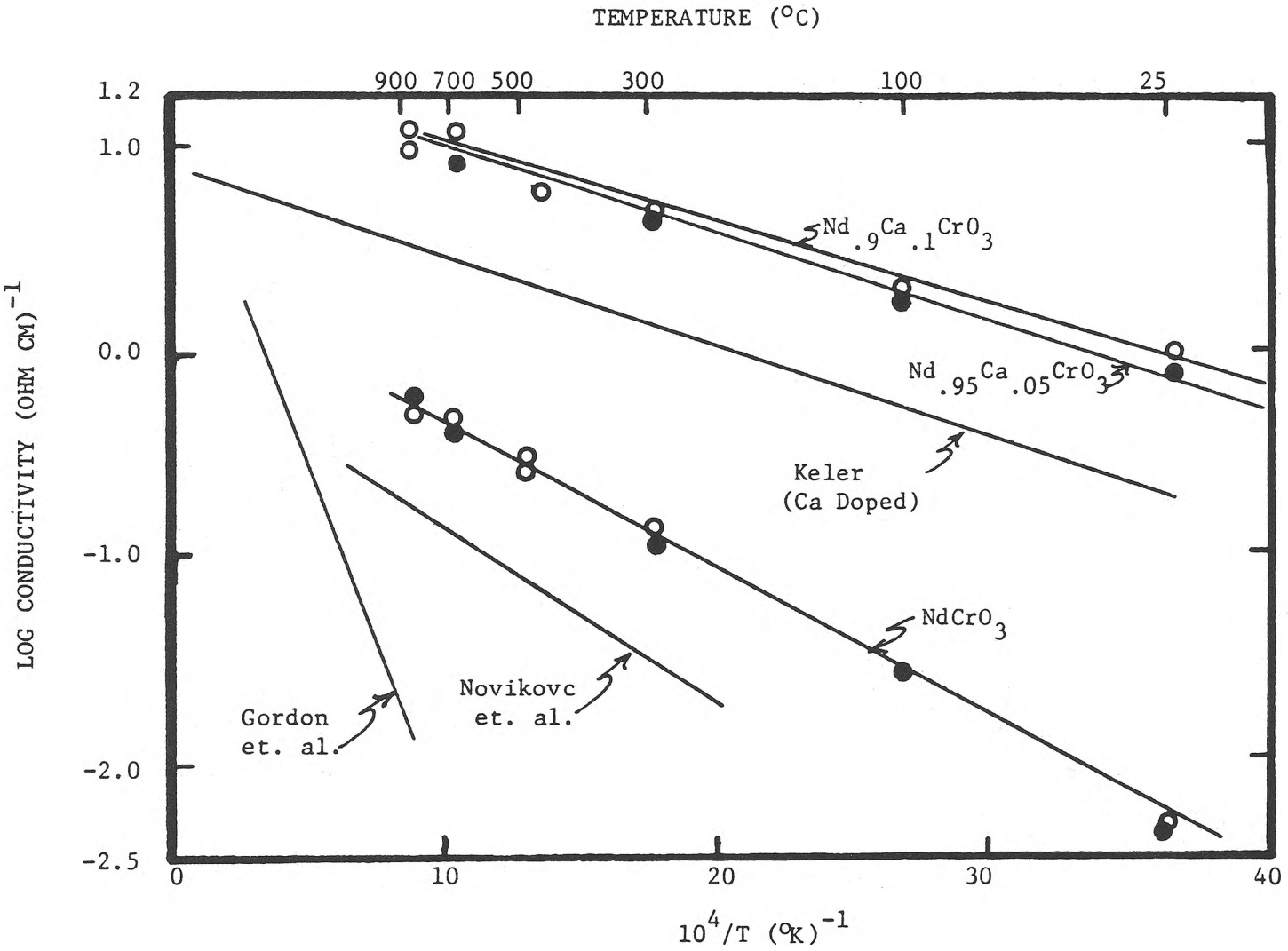

FIGURE 11. TEMPERATURE DEPENDENCE OF CONDUCTIVITY OF $Nd_{1-x}Ca_xCrO_3$

results of Anthony and Foex (1966) and Novikov, Strakov, and Gorbunova (1977) are slightly lower than the data of this study. This is partly because of the correction for porosity. Gordon et. al. (1971) found a much greater slope, showing higher activation energy. Their data was similar to the other data at high temperatures, but at low temperatures conductivity was much lower than that of the other studies. In this study, conductivity varied from 0.0033 $(\text{ohm cm})^{-1}$ at room temperature to 0.39 $(\text{ohm cm})^{-1}$ at 900°C.

Addition of Ca increased the conductivity about two orders of magnitude and decreased the activation energy from 0.14 eV to about 0.08 eV. Figure 11 shows that the conductivities are similar for material with 5% Ca and 10% Ca. Keler (1976) found a lower conductivity for $NdCrO_3$ doped with an unspecified amount of Ca.

In Figure 12, addition of Mg also increased conductivity and reduced activation energy. There is little difference between the materials with 5% and 10% Mg, but the 5% Mg specimen seems to have been a slightly better conductor. It had the highest porosity of any specimen, 36.9%, so this difference could be due to inaccuracies in the correction for porosity. The conductivity and activation energy of $NdCr_{.98}Mg_{.02}O_3$ is between the values for pure $NdCrO_3$ and those for $NdCr_{.95}Mg_{.05}O_3$ and $NdCr_{.9}Mg_{.1}O_3$.

From Table VII, Ca doped materials have slightly higher conductivity and activation energy than Mg doped materials, but the difference is probably not significant. The high conductivity of the doped materials makes them better candidates for MHD electrode materials. The low activation energy is also desireable, because a material with high

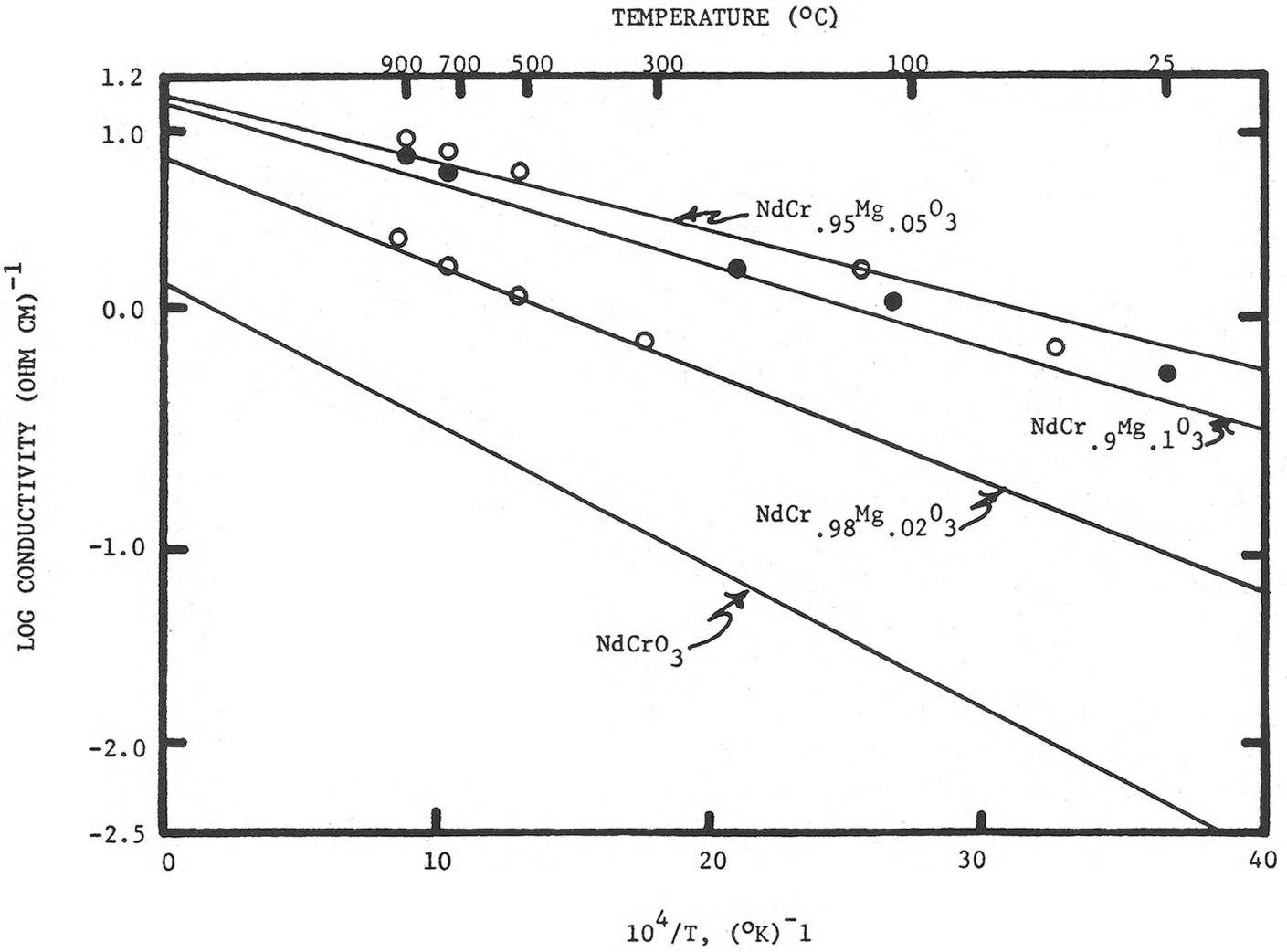

FIGURE 12. TEMPERATURE DEPENDENCE OF CONDUCTIVITY OF $NdCr_{1-x}Mg_xO_3$

activation energy will have low conductivity in the cooler portion of the electrode. Because of its good electrical properties and sintering behavior, the effects of substitution of Al for Cr were investigated for Ca doped $NdCrO_3$ rather than pure $NdCrO_3$.

The conductivity data for $Nd_{.95}Ca_{.05}Cr_{1-x}Al_xO_3$ are plotted in Figure 13. Substitution of 10 or 20 mole percent Al for Cr has almost no effect on σ_o in Table VII, but it reduces E_a, so conductivity is improved. Substitutions of up to 20% Al increased the conductivity, but substitution of 50% Al for Cr decreased conductivity and increased activation energy.

Measurements were made on a specimen of $Nd_{.95}Ca_{.05}Cr_{.95}Fe_{.05}O_3$ with excess Nd before it disintegrated. These data are plotted along with the conductivity data for the new batch with only a slight excess of Nd in Figure 14. The conductivity was not affected by the excess Nd. The variance of the data points from the line was actually less for the combined data from the two specimens than for the specimen with low impurity content alone. For the specimen with low impurity content, $s^2_{x.y}$ from Table VII is 0.0698, but the combined data for the specimen with little excess Nd and the specimen with the high impurity gave $s^2_{x.y} = 0.0508$. The addition of Fe lowered the activation energy, improving the low temperature conductivity, but the high temperature conductivity was slightly reduced.

Several chromites with distorted perovskite crystal structure are being considered for use as MHD electrodes. Conductivity measurements were made on $YCrO_3$, $LaCrO_3$ and Mg doped $LaCrO_3$, Anderson (1980), and the results are shown in Figure 15 along with data for $NdCrO_3$ for

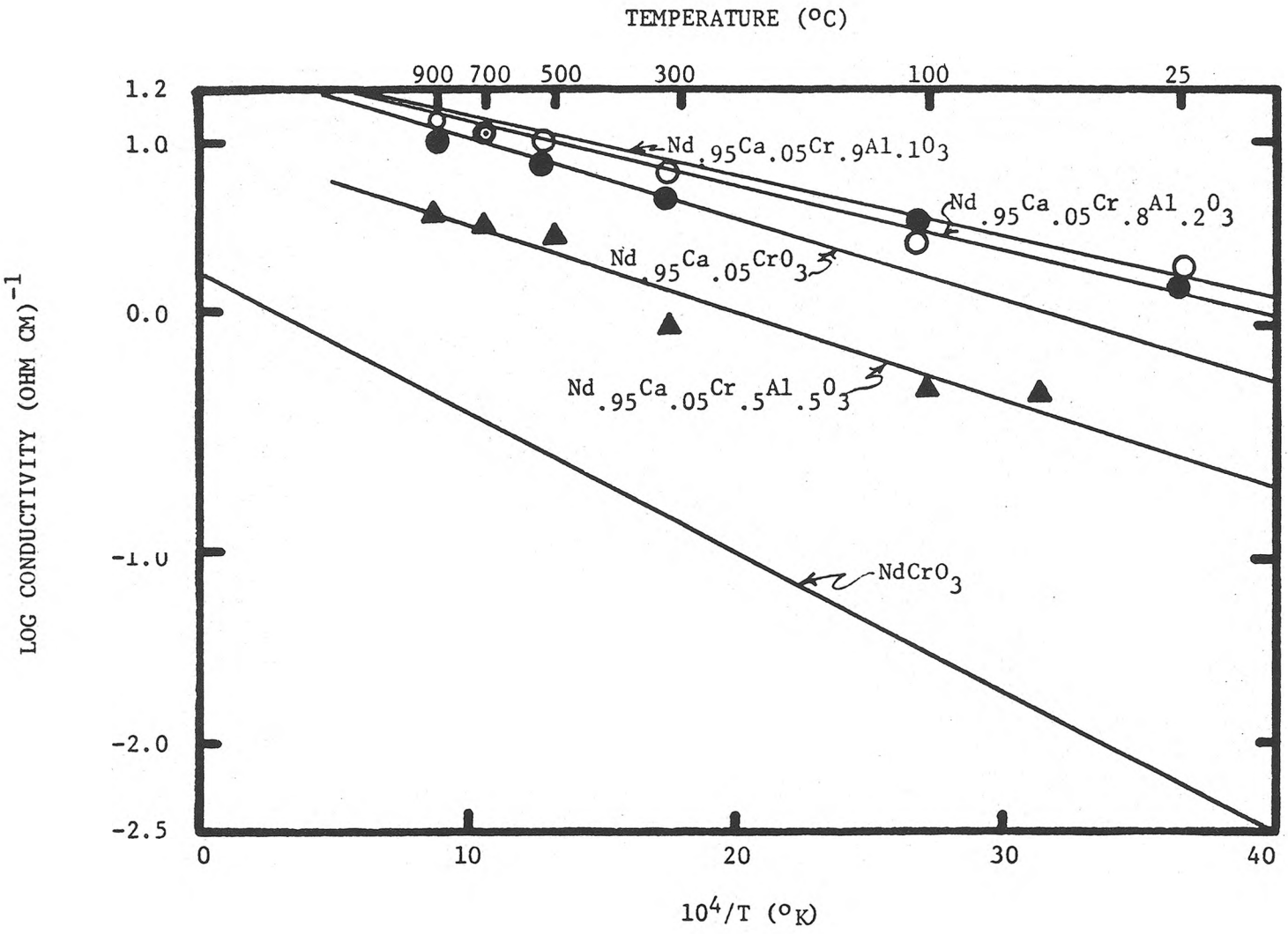

FIGURE 13. TEMPERATURE DEPENDENCE OF CONDUCTIVITY OF $Nd_{.95}Ca_{.05}Cr_{1-x}Al_xO_3$

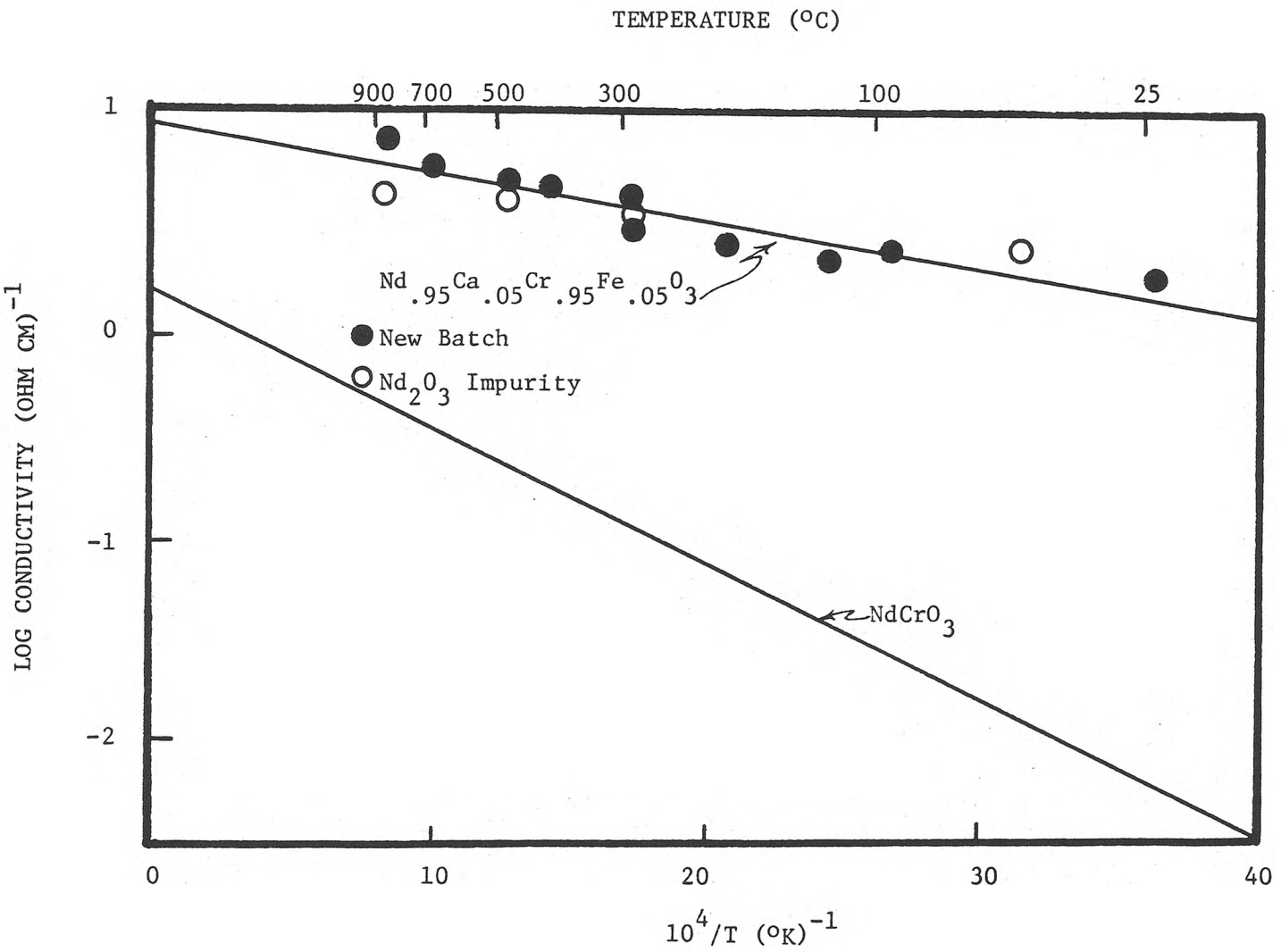

FIGURE 14. TEMPERATURE DEPENDENCE OF CONDUCTIVITY OF $Nd_{.95}Ca_{.05}Cr_{.95}Fe_{.05}O_3$

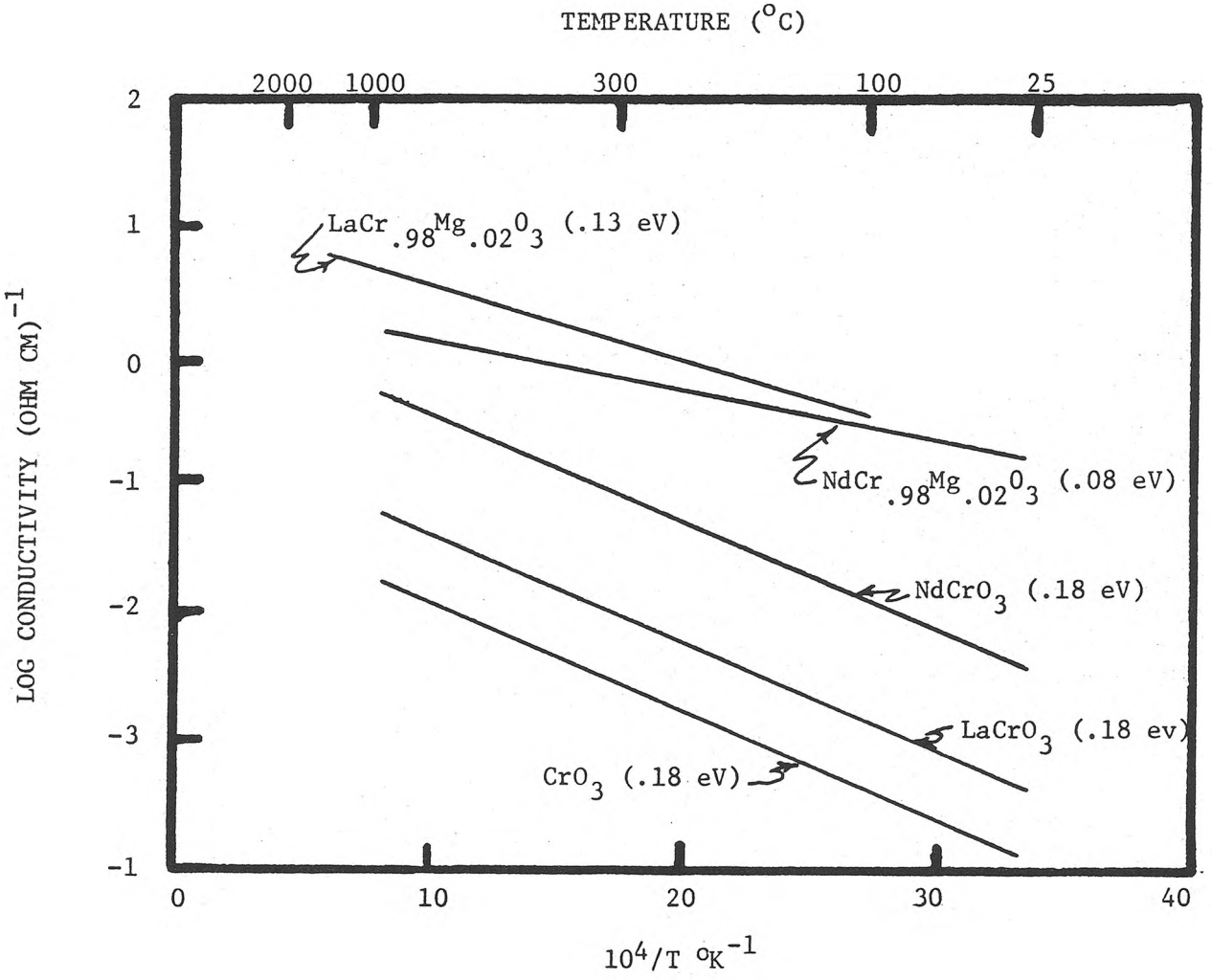

FIGURE 15. TEMPERATURE DEPENDENCE OF CONDUCTIVITY OF VARIOUS CHROMITES

comparison. All three of the chromites have activation energies of 0.18 eV. The conductivity of $YCrO_3$ is the lowest of the three, about 10^{-4} $(ohm\ cm)^{-1}$ at room temperature. $LaCrO_3$ is intermediate with slightly less than 10^{-3} $(ohm\ cm)^{-1}$, and $NdCrO_3$ has the highest room temperature conductivity, about 3×10^{-3} $(ohm\ cm)^{-1}$. The room temperature conductivities of $LaCr_{.98}Mg_{.02}O_3$ and $NdCr_{.98}Mg_{.02}O_3$ are similar, but $LaCr_{.98}Mg_{.02}O_3$ has a higher activation energy (0.13 eV compared to 0.08 eV for $NdCr_{.98}Mg_{.02}O_3$) and higher conductivity at high temperature.

D. THERMAL EXPANSION

Before a layered electrode can be made, the thermal expansion of the $NdCrO_3$ must be matched to that of stabilized ZrO_2, about $10.5 \times 10^{-6}/^{o}C$. In Table VIII, the average thermal expansion coefficient of $NdCrO_3$ in this study was $7.4 \times 10^{-6}/^{o}C$, and Henry and Thompson report $8.3 \times 10^{-6}/^{o}C$. Table VIII gives average thermal expansion coefficients of all the compositions tested. Figure 16 shows that thermal expansion coefficient increased with addition of Ca and Al. Additions of 2 mole percent Mg decreased the thermal expansion coefficient, but further additions of Mg increased the thermal expansion coefficient. Only one Fe doped composition was made, so it was not graphed on Figure 16, but 5 mole percent Fe increased the thermal expansion coefficient to $10.2 \times 10^{-6}/^{o}C$. Thus, if the $NdCrO_3$ is doped with Ca to increase electrical conductivity and Fe so that it can be sintered in air, and if some Al is substituted for Cr, it should be possible to match the thermal expansion coefficient of stabilized ZrO_2. No tests were made on compositions containing both Al and Fe.

TABLE VIII

AVERAGE THERMAL EXPANSION COEFFICIENTS FROM

ROOM TEMPERATURE TO 900°C

Composition	Thermal Expansion Coefficient $^{o}C^{-1}$
$NdCrO_3$	7.38×10^{-6}
$NdCrO_3$ *(Henry and Thompson)	8.31×10^{-6}
$Nd_{.95}Ca_{.05}CrO_3$	7.8×10^{-6}
$Nd_{.9}Ca_{.1}CrO_3$	8.1×10^{-6}
$Nd_{.8}Ca_{.2}CrO_3$	8.7×10^{-6}
$NdCr_{.98}Mg_{.02}O_3$	7.2×10^{-6}
$NdCr_{.95}Mg_{.05}O_3$	7.56×10^{-6}
$NdCr_{.1}Mg_{.9}O_3$	7.8×10^{-6}
$Nd_{.95}Ca_{.05}Cr_{.9}Al_{.1}O_3$	8.0×10^{-6}
$Nd_{.95}Ca_{.05}Cr_{.8}Al_{.2}O_3$	8.37×10^{-6}
$Nd_{.95}Ca_{.05}Cr_{.5}Al_{.5}O_3$	9.33×10^{-6}
$NdAlO_3$ *(Henry and Thompson)	10.1×10^{-6}
$Nd_{.95}Ca_{.05}Cr_{.95}Fe_{.05}O_3$	10.2×10^{-6}

*Henry and Thompson determined thermal expansion coefficients from 25°C to 1000°C.

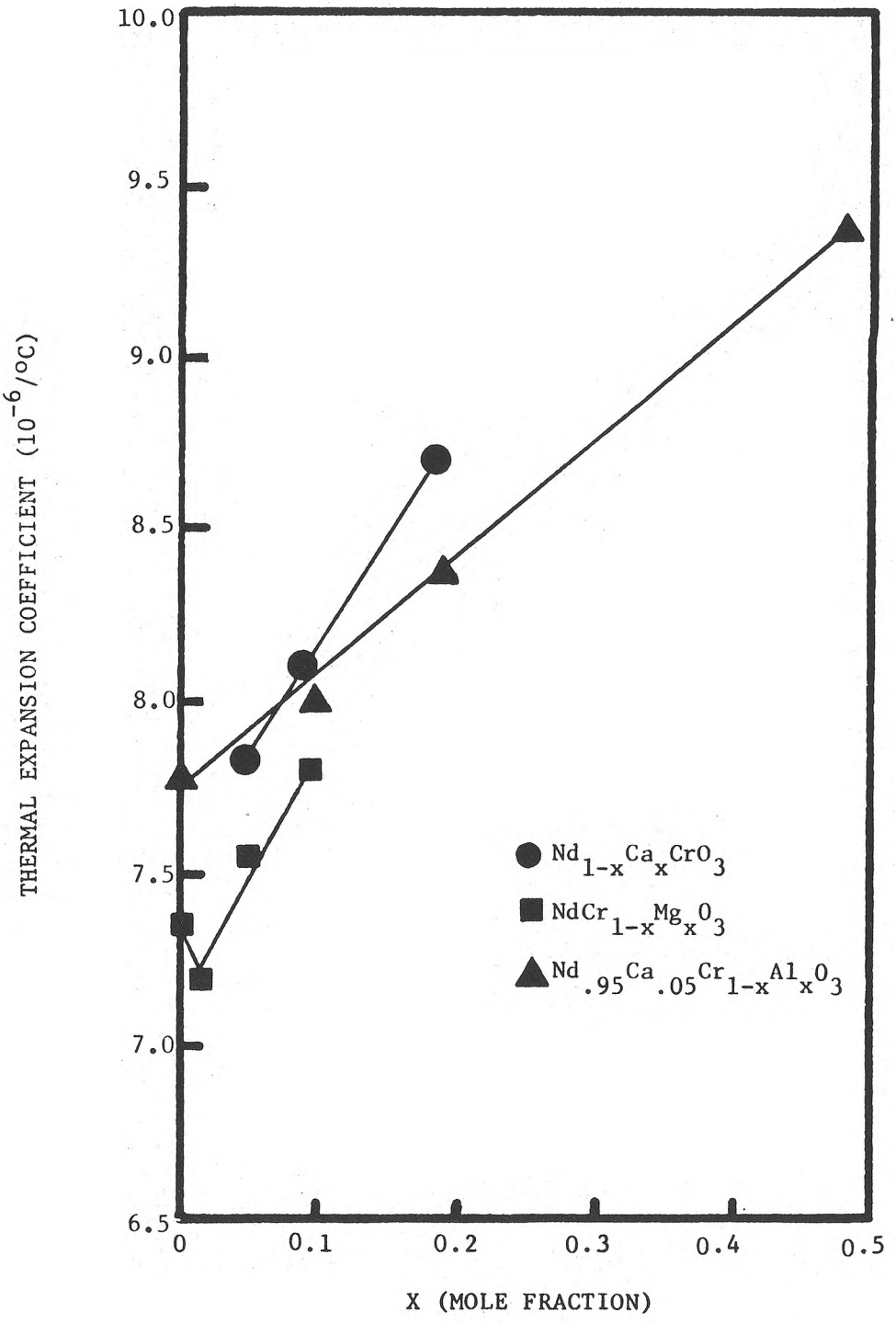

FIGURE 16. VARIATION OF THERMAL EXPANSION COEFFICIENT WITH COMPOSITION

V. CONCLUSIONS

All the compositions were orthorhombic Pbnm with no transformations from room temperature to 900°C.

The compositions can be sintered close to theoretical density in a reducing atmosphere. Addition of 5% Ca prevents exaggerated grain growth. With the addition of 5% Fe for Cr, the material can be sintered in air.

Electrical conductivity of pure $NdCrO_3$ does not meet the goal of 0.5 to 1.0 $(ohm\ cm)^{-1}$, but most of the Ca and Mg doped compositions do have adequate conductivity. They also have low activation energy (~ 0.08 eV).

The thermal expansion coefficients of the compositions vary from $7.2 \times 10^{-6}/°C$ to $10.2 \times 10^{-6}/°C$. Both Fe and Al increased thermal expansion, so it should be possible to find a composition that would match the thermal expansion coefficient of stabilized ZrO_2, about $10.5 \times 10^{-6}/°C$.

The corrosion and erosion requirements are probably the most severe and difficult to meet, and no measurements were made in this area. The material is an electronic conductor, so electrochemical corrosion would be less of a problem. Studies on the corrosion of $NdCrO_3$ under the conditions in the MHD channel would be needed to determine the effects of the various dopants on corrosion resistance, and to determine whether any of the compositions could survive long enough to make a useful electrode.

BIBLIOGRAPHY

Anderson, H.U., "Fabrication and Property Control of $LaCrO_3$ Based Oxides," Proceedings of Crystalline Ceramics, edited by Hayne Palmour III, R.F. Davis and T.M. Hare, Plenium 1978, pp. 469-477.

Anderson, H.U., unpublished research (1980).

Anthony, A.M., and Foex, M., "Insulators and Conductors for MHD Flow," Electricity From MHD, Proceedings of a Symposium, Salzburg, 4-8 July, 1966, International Atomic Energy Agency, Vienna, 1966, Vol. III, pp. 265-281.

Cadoff, L.H., Dilmore, J.A., Lempert, J., Rossing, B.R., Smith, H.D., Turner, A.B. and Young, W.E., "The Design of Electrode Systems and Evaluation of Electrode Materials and Semi-Hot Wall MHD Channels," Ash Deposits and Corrosion Due to Impurities in Combustion Gases, ed. Richard W. Bryers, Hemisphere Publishing Corp., Washington, 1977, pp. 603-626.

Coutures, J.P., Berjoan, R., and Granier, B., "Utilization of Solar Furnaces to Study Interactions Between Gas and Liquid Oxides," Revue Internationale des Hautes Temperatures et des Refractories, X, 4 (1973), pp. 273-281.

Davidge, R.W., Mechanical Behavior of Ceramics. Cambridge: Cambridge University Press, 1979, p. 82.

Foex, Marc, "Oxides with Extremely Good Refractory Properties for use as Magnetohydrodynamic Electrodes," Electricity From MHD, Proceedings of a Symposium, Warsaw, 24-30 July, 1968. International Atomic Energy Agency, Vienna, 1968. Vol. V, pp. 3139-3160.

Geller, S., "Crystal Structure of Gadolinium Orthoferrite, $GdFeO_3$," Journal of Chemical Physics, XXIV, 6 (June, 1956) pp. 1236-1239.

Geller, S., "Crystallographic Studies of Perovskite-Like Compounds. IV. Rare Earth Scandates, Vanadites, Galliates, Orthochromites," Acta Crystallographica, X, (1957) pp. 243-248.

Geller, S. and Bala, V.B., "Crystallographic Studies of Perovskite-Like Compounds. II. Rare Earth Aluminates," Acta Crystallographica, IX, (1956) pp. 1019-1025.

Gordon, V.G., Rekov, A. I., Spiridonov, E.G., and Timofeeva, N.I., "Electrical Resistance of $LaCrO_3$, $NdCrO_3$, $SmCrO_3$, and $YCrO_3$ at High Temperatures," Izv. Akad. Nauk SSSR, Neorg. Mater. VII, 6 (1971) pp. 1084-1085.

Henry, Jack L., and Thompson, Gerald G., "Thermal Expansion Match Between Molybdenum (TZM Alloy) and Oxides of Perovskite and Spinel Types," Ceramic Bulletin, LV, 3 (1976) pp. 281-284.

Keith, M.L., and Roy, Rustum. "Structural Relationships Among Double Oxides of Trivalent Elements," The American Mineralogist, XXXIX, (1954), 1-23.

Keler, E.K., "Development of Physical and Chemical Basis for MHD Generator Oxide Electrode Materials," U.S.-U.S.S.R. Colloq. Magnetohydrodyn. Elec. Power Gener. (Proc.), 3rd (1976) NTIS, Springfield, Va., pp. 405-412.

Mason, T.O., "Materials Problems for Highly Conductive Ceramics in Energy Conversion." Paper read at the Electronics Division of the American Ceramic Society Fall Meeting, September, 1979, Williamsburg, Virginia.

Maxwell, J.C., A Treatise on Electricity and Magnetism, Vol. 1, 3rd ed., Oxford, 1904, p. 441.

Meadowcroft, D.B., "Ceramic Electrodes," Open Cycle M.H.D. Power Generation, ed. Heywood, J.B. and Womack, G.J., Permagon Press, 1969, pp. 532-548.

Novikov, V.K., Strakhov, V., Gorbunova, K.G., "Study of Electrical Conductivity of Stabilized ZrO_2 in Contact with Rare Earth Chromites," Teplofiz. Vys. Temp. XV, 4 (1977) pp. 888-892.

Pavlikov, V.N., Lopato, L.M., and Tresvyatskii, S.G., "Phase Transformations of Some Chromites of Rare Earth Elements," Izv. Akad. Nauk SSSR, Neorg. Mater. II, 4 (1966) pp. 679-680.

Pavlikov, V.N., Shevchenko, A.V., Lopato, L.M., and Tresvyatskii, S.G., "Rare Earth Element Chromites and Their Physicochemical Properties," Khimia Vysokotemperaturnykh Materialov, Tr. Vses. Soveshch., 2nd, Leningrad 1965, pp. 52-59.

Pavlikov, V.N., and Tresvyatskii, S.G., Figure 2361, Phase Diagrams for Ceramists, 1969 Supplement, ed. Levin, E.M., Robbins, C.R., and McMurdie, H.F., American Ceramic Society, Columbus, Ohio, p. 100.

Pechini, M., "Method of Preparing Lead and Alkaline Earth Titanates and Niobates and Coating Method Using the Same to Form a Capacitor," U.S. Patent 3,330,697, July 11, 1967.

Portnoi, K.I., and Timofeeva, N.I. "Physicochemical Properties of High-Melting Oxygen Compounds of Rare Earth Elements," Khimia Vysokotemperaturnykh Materialov, Tr. Vses. Soveshch., 2nd, Leningrad 1965, pp. 48-52.

Quezel-Ambrunaz, S., and Mareschal, M. "Parametres Cristalline des Chromites de Terres Rares," Societe Francaise de Mineralogie et de Cristallographie, Bulletin, LXXXVI, 2 (1963), pp. 204-205.

Remeika, J.P., Growth of Single Crystal Rare Earth Orthoferrites and Related Compounds," American Chemical Society Journal, LXXVIII, (Sept. 5, 1956) pp. 4259-4260.

Robinson, R., "Metal Electrodes," Open Cycle M.H.D. Power Generation, ed. J.B. Heywood and G.J. Womack. Permagon Press, 1969, pp. 506-532.

Schneider, S.J., Roth, R.S., and Waring, J.L., "Solid State Reactions Involving Oxides of Trivalent Cations," Journal of Research of the National Bureau of Standards, 65A, 1961, pp. 345-374.

Stearman, Roebert L., "Statistical Concepts in Microbiology," Bact. Rev., XIX, (1955) pp. 160-215.

Strakhov, V.I., Gorbunova, K.N., Novikov, V.K., and Sergeev, G.G., "Kinetics of Reactions in Mixtures of Components and Phases of the Systems $MgO-Nd_2O_3-Al_2O_3$, $MgO-Nd_2O_3-Cr_2O_3$," Nerganicheskie Materialy, XII, 3 (1976) pp. 439-441.

Toropov, N.A. and Kiseleva, T.P., Figure 2342, Phase Diagrams for Ceramists, 1969 Supplement, ed. Levin, E.M., Robbins, C.R., and McMurdie, H.F., American Ceramic Society, Columbus, Ohio, p. 95.

Wold, A. and Croft, W., "Preparation and Properties of the Systems $LnFe_xCr_{1-x}O_3$ and $LaFe_xCo_{1-x}O_3$," Journal of Physical Chemistry, LXIII, 3 (March, 1959), pp. 447-448.

Yerouchalmi, D., "Introduction," Electricity From MHD, Proceedings of a Symposium, Salzburg, 4-8 July, 1966, International Atomic Energy Agency, Vienna, 1966, Vol. III, pp. 183-191.

Zyrin, A.V., Dubok, V.A., and Tresvyatskii, S.G., "Electrical Properties of Rare Earth Oxides and Some of their Compounds," Khima Vysokotemperaturnykh Materialov, Tr. Vses. Soveshch., 2nd Leningrad, 1965, pp. 52-59.

VITA

David Charles Hitchcock was born on October 31, 1956 in Kansas City, Missouri. He received his primary and secondary education in Independence, Missouri. He attended Longview Community College in Lee's Summit, Missouri, and was awarded the degree of Associate in Engineering in May, 1976. He then attended the University of Missouri-Rolla, and was awarded the degree of Bachelor of Science in Ceramic Engineering in May, 1978. He was then a graduate student at the University of Missouri-Rolla until December, 1979. He is now enrolled in the Graduate School of the University of California, Berkeley.

APPENDIX A

X-RAY DIFFRACTION DATA

The following powder data are from fast scans at 2° 2θ/minute with Ni-filtered Cu Kα radiation. The powder specimens had been annealed at 1400°C for 24 hours.

Relative intensities were determined by measuring the areas under the peaks.

The lattice parameters from Geller (1957) were used to calculate the d spacings of all allowed reflections for pure $NdCrO_3$, and the observed patterns were indexed by comparison to this calculated pattern. The d's were calculated with the equation

$$\frac{1}{d^2} = \frac{h^2}{a^2} + \frac{k^2}{b^2} + \frac{l^2}{c^2}$$

where h, k, and l are the Miller indices of the reflecting plane and a, b, and c are the lattice parameters.

Some peaks should have appeared close to observed peaks. They might have been included with the observed peak, so they were listed enclosed in parentheses.

TABLE IX

CALCULATED X-RAY PATTERN FOR $NdCrO_3$

Plane	d_{calc} (Å)	Plane	d_{calc} (Å)
101	4.427	114	1.721
110	3.856	310	1.714
002	3.847	131	1.692
111	3.447	311	1.673
020	2.747	132	1.581
112	2.723	024	1.576
200	2.706	204	1.568
021	2.587	312	1.566
120	2.450	223	1.541
210	2.428	230	1.517
121	2.334	124	1.513
103	2.318	214	1.508
211	2.315	320	1.508
022	2.236	231	1.488
202	2.213	321	1.480
113	2.136	105	1.480
122	2.066	303	1.476
212	2.053	133	1.437
220	1.928	115	1.429
004	1.924	313	1.425
023	1.875	232	1.411
221	1.870	322	1.404
123	1.771	040	1.374
213	1.763	224	1.361
301	1.756	400	1.353
130	1.735	041	1.352
222	1.724	140	1.331

$NdCrO_3$

Plane	d (Å)	I_{rel}
110 002	3.834	20
111	3.420	5
$Nd(OH)_3$	2.998	3
020 112 200	2.713	100
$Nd(OH)_3$	2.652	2
021	2.567	3
103 211 (121)	2.309	3
022 202	2.227 2.206	13
113	2.127	3
220 004	1.922	25
023 221	1.866	6
222 114	1.719	
131 (310) (311)	1.686	6
132 024 204 312	1.573 1.566	31
133 (151) (313)	1.433	3

$NdCrO_3$ (Con't.)

Plane	d (Å)	I_{rel}
040	1.359	8
224		
400		

$Nd_{.95}Ca_{.05}CrO_3$

Plane	d (Å)	I_{rel}
110 002	3.834	18
111	3.427	5
$Nd(OH)_3$	3.003	5
020 112 200	2.706	100
021	2.564	5
022 202	2.222 2.206	18
220 004	1.918	30
023 221	1.863	9
222 114	1.716	7
131 (310) (311)	1.618	7
132 024 204 312	1.570 1.563	45
133 (151) (313)	1.431	2
040 224 400	1.356	14

$Nd_{.9}Ca_{.1}CrO_3$

Plane	d (Å)	I_{rel}
110 002	3.818	17
111	3.414	3
$Nd(OH)_3$	2.988	6
020 112 200	2.706	100
021	2.564	6
022 202	2.222 2.212	17
113	2.127	3
220 004	1.920	28
023 221	1.866	6
222 114	1.716	6
131 (310) (311)	1.682	6
132 024 204 312	1.573 1.566	45
133 (115) (313)	1.433	3
040 224 400	1.359	17

$Nd_{.8}Ca_{.2}CrO_3$

Plane	d (Å)	I_{rel}
110 002	3.834	13
111	3.427	3
$Nd(OH)_3$	2.998	3
020 112 200	2.706	100
021	2.564	3
022 202	2.222 2.209	15
220 004	1.920	25
023 221	1.864	5
222 114	1.713	5
131 (310) (311)	1.681	5
132 024 204 312	1.563	30
040 224 400	1.356	10

$NdCr_{.98}Mg_{.02}O_3$

Plane	d (Å)	I_{rel}
110 002	3.850	20
111	3.440	5
$Nd(OH)_3$	3.013	3
020 112 200	2.726	110
021	2.581	5
103 211 (121)	2.315	2
022 202	2.233 2.217	20
113 220 004	2.132 1.929	3 30
023 221	1.873	7
222 114	1.725	7
131 (310) (311)	1.692	6
132 024 204 312	1.580 1.570	45
223	1.546	2
133 (115) (313)	1.439	3

$NdCr_{.95}Mg_{.05}O_3$

Plane	d (Å)	I_{rel}
110 002	3.850	20
111	3.440	5
$Nd(OH)_3$	3.008	3
Nd_2O_3	2.885	2
020 112 200	2.722	100
021	2.585	3
103 211 (121)	2.315	2
022 202	2.233 2.222	17
113	2.137	3
220 004	1.931	25
023 221	1.892	5
222 114	1.725	8
131 (310) (311)	1.695	7
132 024 204 312	1.580 1.573	33
133 (115) (313)	1.439	2

$NdCr_{.95}Mg_{.05}O_3$ (Con't.)

Plane	d (Å)	I_{rel}
040	1.364	10
224		
400		

$NdCr_{.9}Mg_{.1}O_3$

Plane	d (Å)	I_{rel}
110	3.867	20
002		
111	3.466	6
$Nd(OH)_3$	3.028	3
020	2.730	100
112		
200		
021	2.592	3
103	2.327	2
211		
(121)		
022	2.249	16
202	2.227	
113	2.146	3
220	1.937	25
004		
023	1.877	6
221		
222	1.728	6
114		
131	1.698	6
(310)		
(311)		
132	1.583	40
024		
204	1.575	
312		
133	1.441	3
(115)		
(313)		
040	1.367	10
224		
400		

$Nd_{.95}Ca_{.05}Cr_{.9}Al_{.1}O_3$

Plane	d (Å)	I_{rel}
110 002	3.850	14
111	3.427	3
$Nd(OH)_3$	3.003	1
020 112 200	2.714	100
021	2.571	3
103 211 (121)	2.309	1
022 202	2.217	20
113	2.127	3
220 004	1.922	20
023 221	1.863	4
222 114	1.719	6
131 (310) (311)	1.684	6
132 024 204 312	1.568	25
133 (115) (313)	1.431	1
040 224 400	1.359	8

$Nd_{.95}Ca_{.05}Cr_{.8}Al_{.2}O_3$

Plane	d (Å)	I_{rel}
110 002	3.818	16
111	3.414	3
$Nd(OH)_3$	2.988	3
020 112 200	2.706	100
021	2.557	2
103 211 (121)	2.304	1
022 202	2.212	12
113	2.122	2
220 004	1.914	16
023 221	1.859	3
222 114 310 131	1.710	4
311	1.674	2
132 024 204 312	1.561	24
115 313	1.425	1
040 224 400	1.356	7

$Nd_{.95}Ca_{.05}Cr_{.5}Al_{.5}O_3$

Plane	d (Å)	I_{rel}
110 002	3.081	14
111	3.401	1
$Nd(OH)_3$	2.978	2
020 121 200	2.694	100
021	2.536	1
120 210	2.433	1
103 211 (121)	2.298	1
022 202	2.196	12
113	2.108	1
220 004	1.905	18
023 221	1.845	2
222 114	1.722	1
131 310 311	1.704	6
123 042 131 310 311	1.664	2
132 024 204 312	1.555	18

$Nd_{.95}Ca_{.05}Cr_{.5}Al_{.5}O_3$ (Con't.)

Plane	d (Å)	I_{rel}
040	1.348	8
224		
400		

$Nd_{.95}Ca_{.05}Cr_{.95}Fe_{.05}O_3$ (Con't.)

Plane	d (Å)	I_{rel}
110 002	3.384	20
111	3.427	7
$Nd(OH)_3$	2.998	4
020 112 200	2.714	100
021	2.571	4
103 211 (121)	2.309	2
022 202	2.227 2.206	18
113	2.127	4
220 004	1.922	30
023 221	1.866	7
222 114	1.716	7
131 (310) (311)	1.684	7
132 024 204 312	1.570 1.563	35
133 (115) (313)	1.429	4
040 224 400	1.357	10

$Nd_{.95}Ca_{.05}Cr_{.95}Fe_{.05}O_3$

Plane	d (Å)	I_{rel}
110 002	3.834	20
111	3.427	7
$Nd(OH)_3$	2.998	4
020 112 200	2.714	100
021	2.571	4
103 211 (121)	2.309	2
022 202	2.227 2.206	18
113	2.127	4
220 004	1.922	30
023 221	1.866	7
222 114	1.716	7
131 (310) (311)	1.684	7
132 024 204 312	1.570 1.563	35
133 (115) (313)	1.429	4
040 224 400	1.357	10

$Nd_{.95}Ca_{.05}Cr_{.95}Fe_{.05}O_3$ (Con't.)

Plane	d (Å)	I_{rel}
116 420	1.211	7

APPENDIX B

ESTIMATES OF ERROR IN THE DETERMINATION OF LATTICE PARAMETERS

The NaCl and $NdCrO_3$ peaks in the slow scans were all analyzed to determine the best estimate of 2θ for the reflection and the highest and lowest possible values of 2θ. These data were used to calculate the highest and lowest possible values of d_{113}, d_{111}, and d_{021}, and also the best estimates of each d. To obtain the best estimates, values of 2θ were obtained from the centers of the peaks at half their heights. The peaks were often asymmetrical, so this point was not in general the highest point on the peak. The same method was used in all determinations in order to get reproducible results. Some of the peaks were flat or rounded at the top rather than sharp, so the maximum and minimum 2θ's were taken from the points where the intensity began to fall off rapidly at the edge of the peak. The choice of maximum and minimum points was somewhat arbitrary, and probably not as reproducible as the choice of the best estimate.

A sample calculation for the highest, lowest, and best values of the lattice parameter c of $NdCrO_3$ is given below. This calculation involves only d_{113} and d_{111}. Calculation of a and b required a third d, d_{021}, but the method used was the same.

First the 2θ's for the 111 and 113 peaks, and for the NaCl peaks used to index them were measured.

Observed 2θ

Peak	Minimum	Best	Maximum	Accepted
113	42.36	42.39	42.42	-------
NaCl	45.53	45.53	45.555	45.47
111	25.865	25.89	25.90	-------
NaCl	27.42	27.42	27.425	27.37

Corrected values of 2θ were calculated by adding correction terms to the observed 2θ's. The correction term for the minimum value of $2\theta_{113}$ is the difference between the accepted value for NaCl and the maximum NaCl 2θ, 45.47 - 45.555 = -0.085. The correction for the best estimate is the difference between the accepted value for NaCl and the best estimate for NaCl, and the correction term for the $NdCrO_3$ maximum is the difference between the accepted and minimum values for NaCl.

Corrected 2θ

Peak	Minimum	Best	Maximum
113	42.275	42.33	42.36
111	25.81	25.84	25.85

When the correction terms are chosen in this way, the maximum error is calculated.

The d values were calculated by Bragg's law.

$$d = \frac{\lambda}{2 \sin \frac{2\theta}{2}} \qquad \lambda = 1.54178\text{Å (Cu K}\alpha)$$

hkl	d_{msc}	d	d_{min}
113	2.1378Å	2.1351Å	2.1337Å
111	3.4517	3.4478	3.4465

The equations

$$1/d_{111}^2 = 1/a^2 + 1/b^2 + 1/c^2$$

and $$1/d_{113}^2 = 1/a^2 + 1/b^2 + 9/c^2$$

were combined to get

$$c = \sqrt{8}\ (1/d_{113}^2 - 1/d_{111}^2)^{-1/2}$$

The maximum value of c was calculated from the maximum value of d_{113} and the minimum value of d_{111}, and the minimum value of c was calculated from the minimum value of d_{113} and the maximum value of d_{111}. The results are:

$$c_{min} = 7.678\text{Å},\ c_{best} = 7.690\text{Å},\ c_{max} = 7.709\text{Å} \quad \text{or} \quad c = 7.690^{+.019}_{-.012}.$$

The length of the interval in which c lies in 7.709 - 7.678 = 0.031Å. The length of this interval gives an estimate of the accuracy of the lattice parameter determinations.

It was also desired to obtain an estimate of the precision, so s^2 was calculated for each of the three lattice parameters from the observed values for $NdCrO_3$, $NdCr_{.98}Mg_{.02}O_3$, $NdCr_{.95}Mg_{.05}O_3$, and $NdCr_{.9}Mg_{.1}O_3$. The lattice parameters in Figure 4 do not appear to change with substitution of Mg for Cr, so the four values for c were assumed to be a sample from the population of experimental values for c, and s^2 was calculated to estimate the variance of the experimental values. (Stearman, 1955)

$$s^2 = \frac{\sum_{i=1}^{n} (X_i - \bar{X})^2}{n-1}$$

X_i is the ith experimental lattice parameter

$\bar{X}$ is the mean of the X_i values,

$$\bar{X} = \frac{\sum_{i=1}^{n} X_i}{n}$$

n is the number of experimental values.

Calculations of s^2 were made for a, b, and c from the data for $NdCr_{1-x}Mg_xO_3$ in Table IV, and the results are given in Table V.

As can be seen in Figure 3, the lattice parameters decrease in a linear fashion as Ca is added, so the standard error of estimate was calculated for the regression lines for the lattice parameters as a function of Ca content. The standard error of estimate, $s^2_{y.x}$ is

$$s^2_{y.x} = \frac{1}{N-2} \Sigma\, Y_i - \{[\bar{Y} + b\,(X_i - X)]\}^2$$

N is the number of pairs of Ca contents and lattice parameters,

$\bar{Y}$ is the mean of the lattice parameters,

Y_i is the ith lattice parameter,

X_i is the corresponding Ca content,

$\bar{X}$ is the mean of the Ca contents,

b is the slope of the regression line, given by

$$b = \frac{\Sigma X_i Y_i - \frac{\Sigma X_i \Sigma Y_i}{N}}{\Sigma X_i^2 - \frac{(\Sigma Xi)^2}{N}}$$

$s^2_{y.x}$ was calculated for each of the lines in Figure 3 using the data from Table IV, and the results are given in Table V.

A 95% confidence interval for the lattice parameters of $NdCrO_3$ and Mg doped $NdCrO_3$ was calculated from the formula

$$\bar{x} - t_{.975}\sqrt{s^2/n} < \mu < \bar{x} - t_{.025}\sqrt{s^2/n}$$

from Stearman. (1955)

$\bar{x}$ is the mean of the experimental values of the lattice parameter for which the confidence interval is being calculated, $t_{.975}$ and $t_{.025}$ come from tables of the t distribution, and these tables can be found in the CRC Handbook, or most statistics texts.

s^2 is the estimate of the variance calculated earlier,

n is the number of x values used in the calculation,

μ is the true lattice parameters.

These confidence intervals are given in Table V.